



# Pseudolesions in the Cirrhotic Liver

Rita Golfieri, Stefano Brocchi, Matteo Milandri,  
and Matteo Renzulli

## Contents

1	<b>Introduction</b> .....	230
2	<b>Technical Pitfalls</b> .....	230
3	<b>Regenerative Nodules and Siderotic Nodules</b> .....	230
4	<b>Perfusion Defects Due to Third Inflow</b> .....	237
5	<b>Transient Hepatic Attenuation Difference (THAD) and Transient Hepatic Intensity Difference (THID)</b> .....	239
5.1	Hepatic Inflow Disorders .....	240
5.2	Hepatic Outflow Disorders .....	247
6	<b>Hemangioma in Cirrhosis</b> .....	248
6.1	Fast-Filling Hemangiomas .....	248
6.2	Sclerosed Hemangiomas .....	250
7	<b>Pseudomass in Cirrhosis and Chronic Portal Vein Thrombosis (PVT)</b> .....	253
8	<b>Confluent Fibrosis</b> .....	254
9	<b>Focal Fatty Changes</b> .....	258
	<b>References</b> .....	263

## Abstract

This chapter analyses the different benign liver lesions and pseudolesions occurring in cirrhotic livers, such as regenerative nodules

(RNs), siderotic nodules (SNs), nodular regenerative hyperplasia (NRH), large regenerative nodules (LRNs), perfusion defects and transient hepatic attenuation difference (THAD)/transient hepatic intensity difference (THID), hemangiomas in a cirrhotic liver, pseudomass in chronic portal vein thrombosis (PVT), confluent fibrosis and focal fatty changes, such as focal steatosis and fat sparing, focusing on imaging features helpful in achieving a correct diagnosis.

R. Golfieri (✉) · S. Brocchi · M. Milandri · M. Renzulli  
Radiology Unit, Department of Experimental,  
Diagnostic and Speciality Medicine,  
Sant'Orsola Hospital, University of Bologna,  
Bologna, Italy  
e-mail: [rita.golfieri@unibo.it](mailto:rita.golfieri@unibo.it)

## 1 Introduction

Cirrhosis is end-stage chronic liver disease and is characterized pathologically by innumerable regenerative nodules separated by fibrous septa (Vilgrain et al. 2016). Cirrhosis is considered to be one of the leading causes of death having a 1-year mortality rate of up to 57% in cases of decompensated cirrhosis (D'Amico et al. 2006). Chronic hepatitis B or C virus infection, alcoholism and non-alcoholic fatty liver disease (NAFLD) are the most common causes of cirrhosis (Brancatelli et al. 2007).

Hepatocellular carcinoma (HCC) is the most common primary tumour in cirrhotic livers, the second leading cause of cancer-related mortality worldwide and the third most common cause of death in patients with cirrhosis (D'Amico et al. 2006; Mittal and El-Serag 2013). Unfortunately, HCC is not rare in cirrhotic patients, with a fairly constant rate of approximately 3% per year, regardless of the cirrhotic stage (D'Amico et al. 2006).

Nevertheless, several other benign and malignant lesions can occur in cirrhotic patients, they should be differentiated from HCC (Brancatelli et al. 2003) in order to minimize both false-negative and false-positive findings, to carry out the proper treatment and, therefore, to improve patient outcome (Galia et al. 2014). The treatment could be erroneously delayed in cases of undetected or misdiagnosed HCC. Misinterpretation of pseudolesions or benign liver lesions, such as HCC, may incorrectly increase the total tumour burden or even lead to the ineligibility of a patient for potentially curative treatment or the inappropriate assignment of increased priority scores for patients on the waiting list for liver transplantation (Galia et al. 2014).

In recent years, magnetic resonance imaging (MRI) has been confirmed to be the most accurate imaging method for the study of the liver. The introduction of hepatocyte-specific contrast agents in MRI, such as gadoxetic acid (Gd-EOB-DTPA, Primovist, Bayer-Schering Pharma, Berlin, Germany) and gadobenate dimeglumine (Gd-BOPTA, Multihance, Bracco Imaging,

Milan, Italy), has added new diagnostic functional parameters to those obtained in the dynamic vascular phases by also evaluating the hepatobiliary (HB) phase of MRI and, therefore, the hepatocyte presence and activity. Moreover, the addition of diffusion-weighted imaging (DWI) sequences can additionally confirm or exclude malignancy in the majority of lesions.

Despite these recent technical innovations in liver imaging, there are still many challenges for radiologists in differentiating HCC from other hepatic lesions, particularly from benign ones and pseudolesions.

---

## 2 Technical Pitfalls

Hypervascular tumours, such as HCC, require adequate delivery of contrast media to create a satisfactory contrast between the tumour and the background liver parenchyma. The rate of contrast injection can affect the tumour-to-background contrast ratio; therefore, the use of an adequately high injection rate is important in order to avoid missing lesions. Moreover, correct acquisition during the late arterial phase is particularly important since this is a unique non-repeatable phase. The American College of Gastroenterology guidelines recommend a minimum flow rate of 4–6 cm<sup>3</sup>/s to obtain a correct examination (Marrero et al. 2014). A slower rate of infusion of 2.5 cm<sup>3</sup>/s may result in suboptimal enhancement, not useful in differentiating lesions from the surrounding hepatic parenchyma.

---

## 3 Regenerative Nodules and Siderotic Nodules

Liver cirrhosis is characterized by irreversible remodeling of the hepatic architecture with bridging fibrosis and a spectrum of hepatocellular nodules. Cirrhosis-associated hepatocellular nodules result from the localized proliferation of hepatocytes and their supporting stroma in response to liver injury (International Working Party 1995). The majority of hepatocellular nodules are benign regenerative nodules; however,

regenerative nodules may progress along a well-described carcinogenic pathway to become low-grade and high-grade dysplastic nodules evolving into hepatocellular carcinoma (HCC) (Hanna et al. 2008).

*Regenerative nodules* (RNs) are classified, according to their size, as micronodules (<3 mm) and macronodules ( $\geq 3$  mm) (International Working Party 1995; Hanna et al. 2008). On computed tomography (CT) and MRI, RNs typically appear isodense/isointense to the surrounding liver parenchyma without arterial phase enhancement or washout appearance and, therefore, they are identifiable due to the peripheral fibrosis which appears hypodense in the portal phase. On MRI, RNs can appear hypointense on T2-weighted images unlike HCC which classically appears moderately hyperintense on T2-weighted images (Elsayes and Shaaban 2015; Hussain et al. 2002).

Some RNs could demonstrate hyperintensity on T1-weighted images and iso- or hypointensity on T2-weighted images (Fig. 1) (Hanna et al. 2008; Martin et al. 2002). Although the reason for these signal intensity (SI) findings is not well understood, the presence of paramagnetic materials or glycogen in the nodule may contribute to T1 hyperintensity (Mathieu et al. 1997). Regenerative nodules may also contain some degree of lipid accumulation in the hepatocytes. Lipid-containing RNs display signal loss on out-of-phase T1-weighted images in comparison with in-phase images (Fig. 2). Steatotic RNs are usually multiple; a single fatty nodule is suggestive of a dysplastic or malignant process (Hanna et al. 2008).

*Siderotic nodules* (SNs) are iron-containing nodules which develop in a cirrhotic liver (Mitchell et al. 1991).

Even in the absence of systemic iron storage diseases such as hemochromatosis, iron can accumulate within regenerative or dysplastic nodules (DNs) in a cirrhotic liver (Zhang and Krinsky 2004). In systemic iron storage diseases, the mechanism of iron deposition (siderosis) within reticuloendothelial cells, mobilizing iron from damaged hepatocytes, has been identified; however, in a cirrhotic liver, the process of SN

formation remains uncertain. Active viral replication and transferrin receptor abnormalities probably play a role. Although a small percentage of SNs are dysplastic, approximately 25% of all DNs are also SNs (Elsayes and Shaaban 2015; Terada and Nakanuma 1989). Moreover, dysplastic SNs are premalignant lesions while regenerative SNs are markers for severe viral or alcoholic cirrhosis. Therefore, the diagnosis of iron content is clinically important. The relationships between hepatic iron deposition and hepatic fibrosis, cirrhosis and neoplasia are also not fully understood (Krinsky et al. 2001; Breitkopf et al. 2009).

Magnetic resonance imaging is currently unable to differentiate siderotic RNs from siderotic DNs (Krinsky et al. 2000), and the association of SNs and malignancy remains controversial. According to some published series, patients with SNs do not show an increased risk of developing DN or HCC (Zhang and Krinsky 2004; Krinsky et al. 2002), but other authors have reported that SN can be precursors of HCC in patients with chronic liver diseases (Terada et al. 1990; Siegelman et al. 1996; Ito et al. 1999) and that the incidence of HCC is higher in patients with iron-containing nodules than in those without (Krinsky et al. 2000). Whenever iron-free foci are found within an SN in liver cirrhosis, these foci should be considered as early HCCs or borderline lesions showing an expansive growth pattern (Zhang and Krinsky 2004); the finding of the displacement of iron within a nodule by focal tumour growth is a sentinel of HCC (Elsayes and Shaaban 2015; Krinsky et al. 2001; Sadek et al. 1995). Therefore, the diagnosis of SNs and iron-free nodules in the cirrhotic liver is clinically relevant for the early detection of HCC.

On CT, SNs occasionally show high attenuation on unenhanced images which can be misinterpreted on the arterial phase as lesion hyperenhancement. In these nodules, both arterial hyperenhancement and washout are absent. Therefore, only the combined evaluation of unenhanced images and post-contrast behaviour allows the proper characterization of SNs.

On MRI, SNs usually appear hypointense on T1-weighted images, depending on the degree of iron accumulation and the exact

imaging parameters (Fig. 3) (Siegelman and Chauhan 2014). Furthermore, SNs have decreased SI in long-echo chemical-shift gradient-echo sequences. A pitfall of MRI is misinterpreting susceptibility from iron content

within SNs as areas of washout appearance (Brancatelli et al. 2007); therefore, it is important to evaluate the unenhanced T1- and T2\*-weighted images in which SNs appear hypointense. T2\*-weighted imaging is

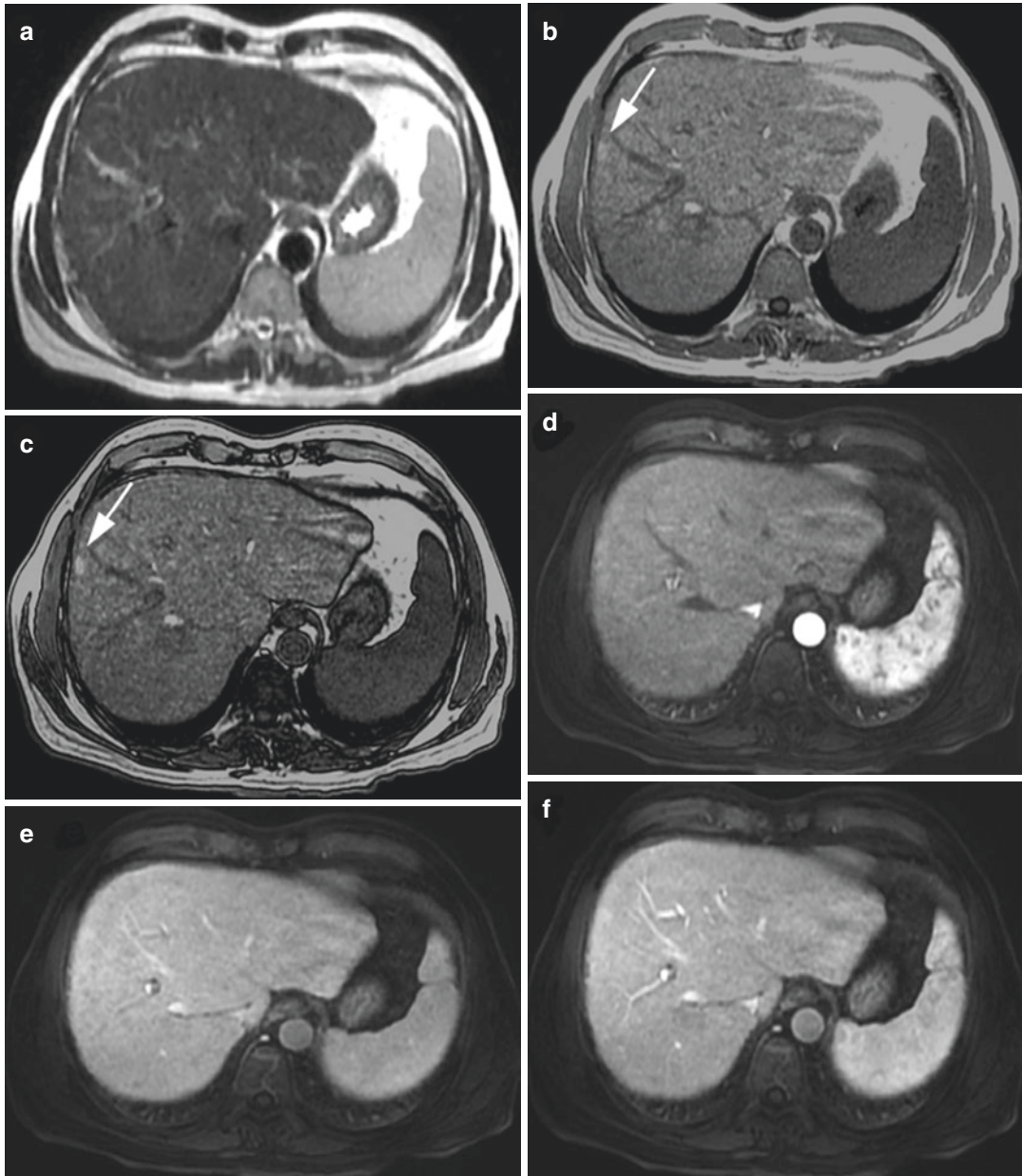


**Fig. 1** Regenerative nodule with glycogen content on MRI. T2-weighted image (a) demonstrating the absence of focal lesions. T1-weighted “in-phase” (b) and “out-of-phase” (c) images showing a hyperintense nodule in liver

segment VIII (arrows), as a result of the glycogen content, with no changes during arterial (d), portal (e), delayed (f) and hepatobiliary (g) phases. Diffusion-weighted image (h) revealing no diffusion restriction of the nodule

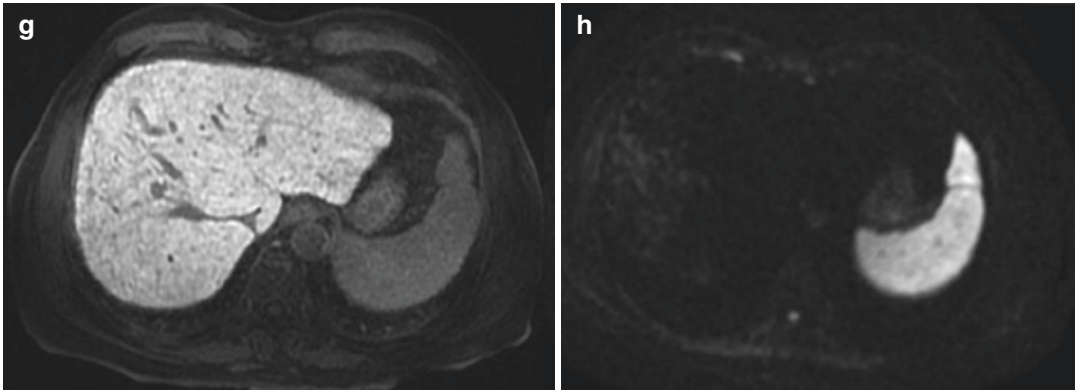


Fig. 1 (continued)

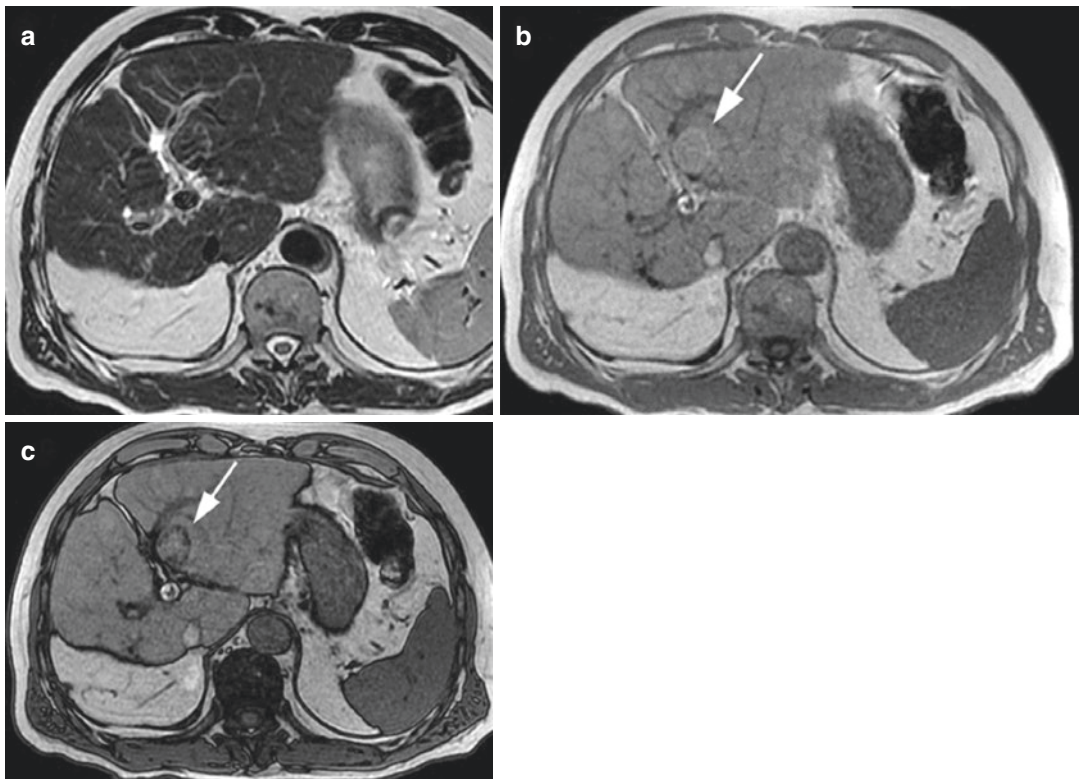


Fig. 2 Regenerative nodule with fat content on MRI. T2-weighted image (a) demonstrating a round isointense focal lesion in segment II. T1-weighted “in-phase” (b) and “out-of-phase” (c) images revealing a

hyperintense nodule (arrows) at segment II with dropout in signal intensity in “out-of-phase” images, due to conspicuous fat content

currently the most sensitive MRI technique for detecting SN in the liver having a reported 80% sensitivity and 95% specificity. MRI is therefore helpful in the follow-up in monitor-

ing the distribution and the amount of iron content over time: this could allow the detection of early HCC developing within a DN (Kudo 2009; Park and Kim 2011; Chen et al. 2012).

Severe long-standing portal deprivation with portal obliterative changes, as observed in chronic PVT, or in cases of venous outflow obstruction, such as in Budd–Chiari Syndrome, produce a progressive and reactive compensatory increase in

hepatic arterial perfusion (“arterial buffer response”), causing the secondary onset of nodular regenerative hyperplasia (NRH) of the liver tissue (Cazals-Hatem et al. 2003) and large regenerative nodules (LRNs, also called focal

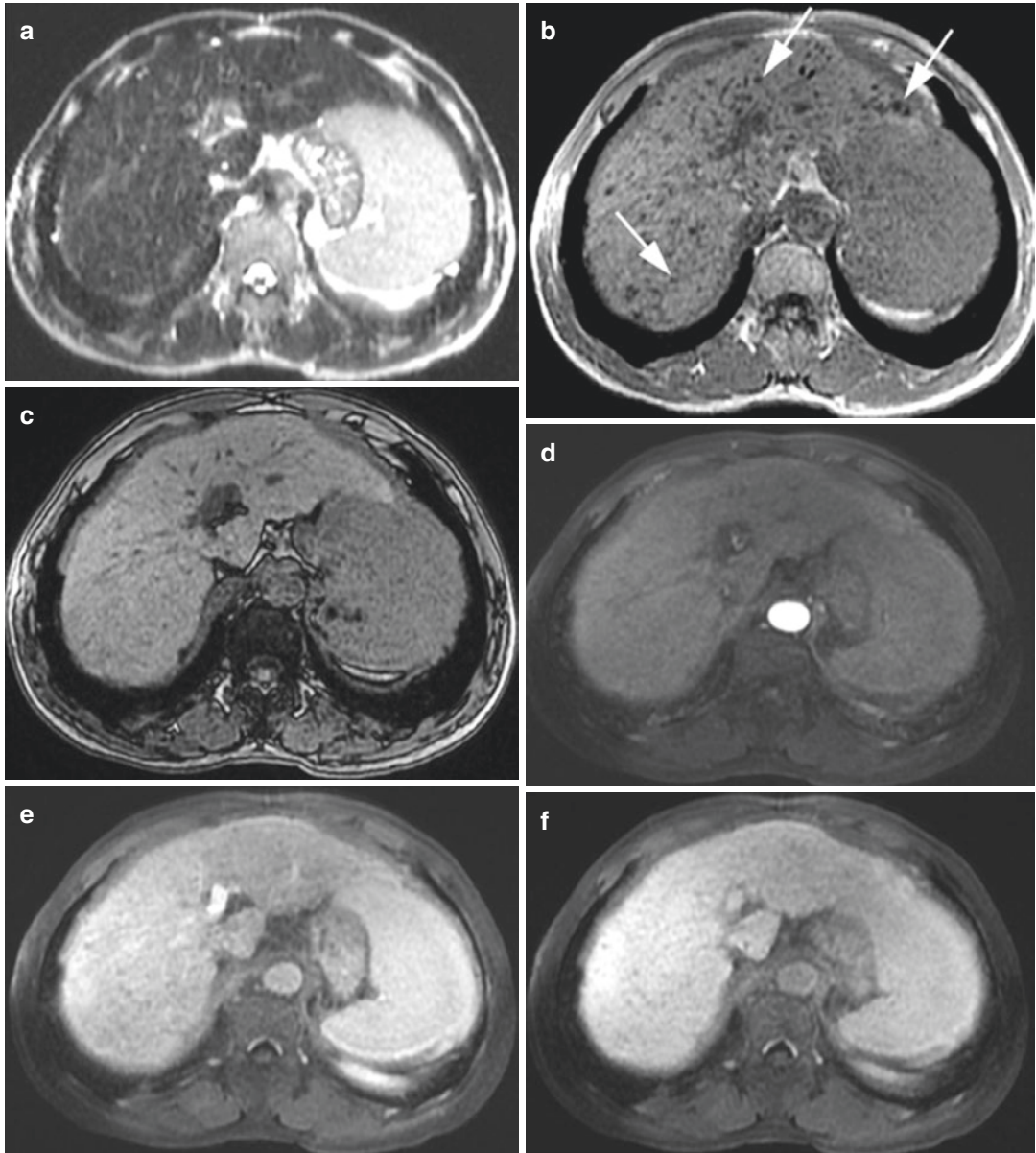


**Fig. 3** Multiple siderotic nodules on MRI. T2-weighted image (a): no evidence of focal lesions. T1-weighted “in-phase” image (b) showing multiple tiny hypointense nodules (arrows) due to their siderotic content, appearing isointense on the T1-weighted “out-of-phase” image (c),

with no changes during the arterial (d), portal (e), delayed (f) and hepatobiliary (g) phases. Diffusion-weighted image (h) revealing the absence of diffusion restriction of the nodules

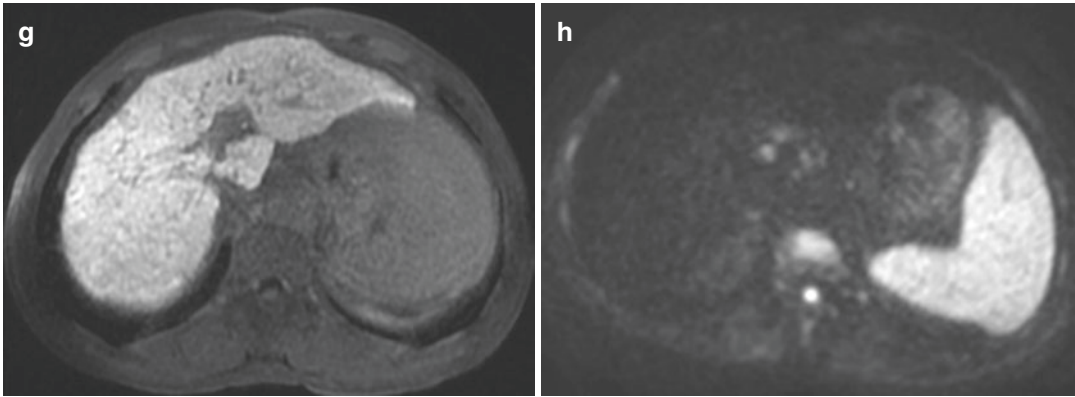


**Fig. 3** (continued)

nodular hyperplasia (FNH)-like lesions (Kondo 2001; Brancatelli et al. 2002a, b). In the same liver, a continuous spectrum of nodular regenerative lesions, such as *NRH and LRNs* (Park and Kim 2011; De Sousa et al. 1991), always coexists. Their pathogenesis is similar to FNH development as proposed by Wanless et al. (1985) in livers with syndromic vascular malformations, leading to portal deprivation and subsequent enlargement of the hepatic artery. In support of the vascular pathogenetic hypothesis, Steiner et al. also noted that NRH is frequently associated with severe congestive heart failure, hypothesizing that patients with cardiovascular disease, especially right heart failure, could develop liver NRH as a consequence of venous outflow impairment, sinusoidal–portal flow reduction and compensatory increase in the hepatic arterial flow (Steiner 1959).

According to the International Working Party classification (International Working Party 1995), NRH is defined as monoacinar nodules, undetectable at imaging, unlike multiacinar nodules, such as LRNs, clearly identified on both CT and MRI.

Nodular regenerative hyperplasia is a benign liver disease, macroscopically characterized by multiple small regenerative nodules of variable dimensions, ranging from 1 to 15 mm. The main cause of NRH is a normal liver with blood flow disturbance (also due to myeloproliferative and rheumatologic disease, organ transplantation and classes of drugs). In patients with NRH, unlike LRNs, no enhancing liver lesions can be detected on imaging (Ames et al. 2009).

Large regenerative nodules are benign multiacinar regenerative nodules, usually multiple, containing more than one portal tract, located in a liver which is otherwise abnormal, either with cirrhosis or with severe portal vein disease, hepatic veins or sinusoids. Large regenerative nodules are distinctly larger than the majority of cirrhotic nodules in the same liver, at least 5 mm in diameter (International Working Party 1995). They are also associated with some systemic disease, such as chronic vascular disease (polyarteritis nodosa), rheumatologic disease (Felty syndrome, rheumatoid arthritis, scleroderma, telangiectasia), systemic lupus erythematosus, lymphoproliferative disorder (Hodgkin lymphoma and non-Hodgkin lymphoma, chronic lymphocytic leukemia), myeloproliferative disorder (polycythemia vera, chronic myeloid leukemia, myeloid metaplasia), hepatic vascular disease (Budd Chiari syndrome, sinusoidal obstruction syndrome) and drugs (steroids, chemotherapy, immunosuppressors and contraceptives) (Wanless 1990; Stromeyer and Ishak 1981). In contrast to NRH, LRNs are clearly depicted at imaging since, on MRI, they appear hyperintense to the liver in T1-weighted images due to the presence of copper within the nodules, and isointense or hypointense on T2-weighted images (Wanless et al. 1990). On post-contrast CT and MRI, LRNs typically enhance in the arterial phase and might potentially be misdiagnosed as HCCs; the differential diagnosis relies on the persistent enhancement

in the portal and delayed phases with absent washout in LRN unlike HCC (Vilgrain et al. 1999; Takayasu et al. 1994). However, there is little evidence to suggest that LRNs are pre-malignant or evolve into HCC (Stromeyer and Ishak 1981). In the HB phase of MRI, hyper-

plastic hepatocytes, such as those in LRNs which often contain ductular proliferation (Tanaka and Wanless 1998), appear isointense or more often hyperintense as compared to the normal parenchyma, unlike HCC (Fig. 4) (Renzulli et al. 2011).

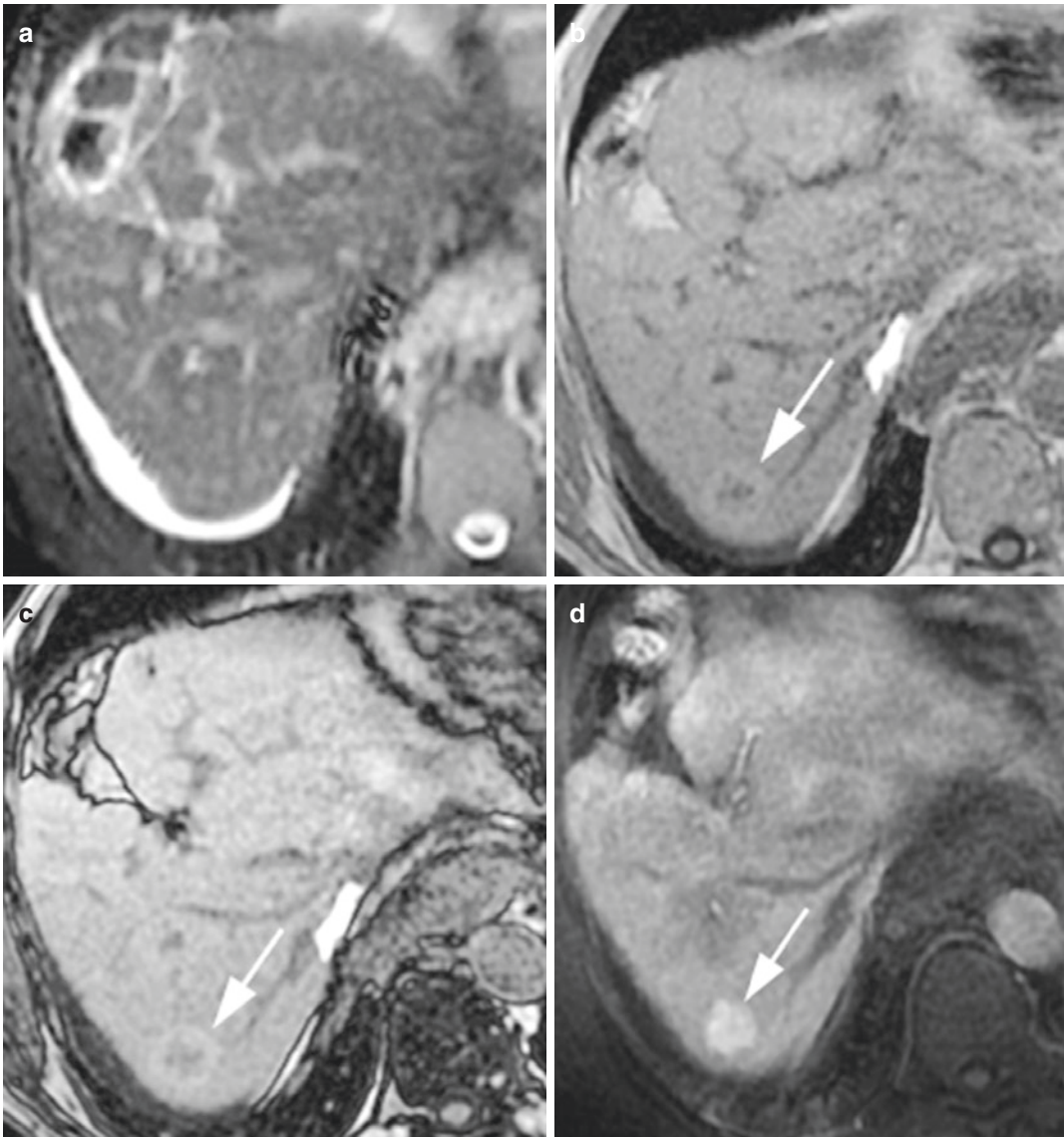


**Fig. 4** Large regenerative nodule on MRI. T2-weighted image (a) demonstrating no hyperintense focal lesions. T1-weighted “in-phase” (b) and “out-of-phase” (c) images revealing a hyperintense nodule at segment VII

(arrows). Arterial phase (d) showing nodule hyperenhancement, persistent (arrows) during the portal phase (e), additionally increasing in the hepatobiliary phase (arrow) (f)



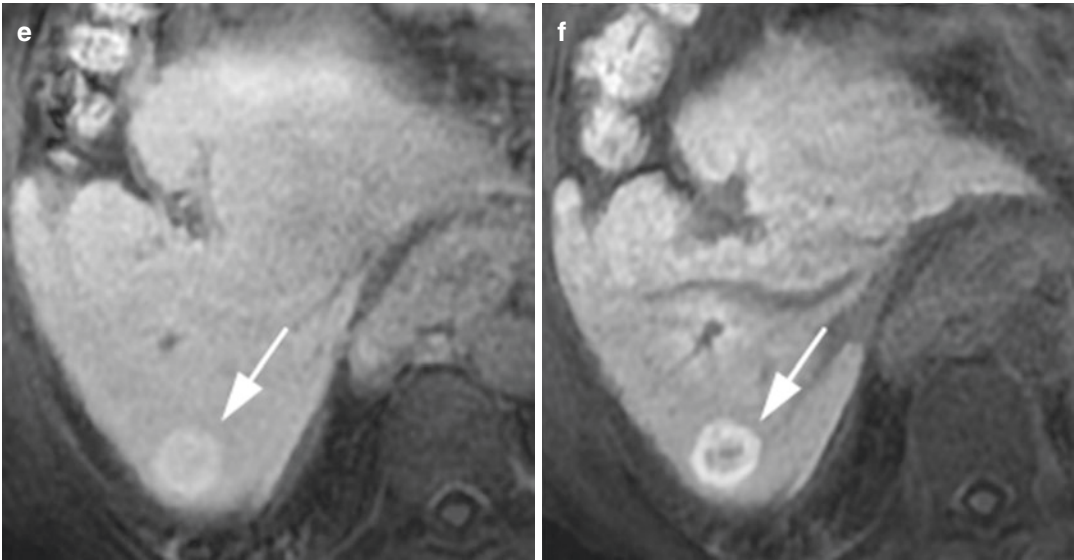


**Fig. 4** (continued)

#### 4 Perfusion Defects Due to Third Inflow

The third inflow is a non-portal blood venous system with hepatopetal flow. This system vascularizes some parenchymal regions of the liver and deprives these districts of the nutritional contents deriving from the absorption of the small intestine which characterizes the portal blood. The third inflow represents approximately 1–5% of the total liver inflow and includes the following veins (Fig. 5) (Itai and Matsui 1999; Couinaud 1988; Yoshimitzu et al. 2001; Kobayashi et al. 2010):

- (a) Cholecystic vein branches which penetrate the hepatic parenchyma in segments IV and V and flow into the parabiliary system at the porta hepatis. They drain the gallbladder and extrahepatic bile ducts.
- (b) Parabiliary venous system (Couinaud system) is a network of venules which goes up to the hepatic hilum, near the hepatoduodenal ligament and the main portal trunk, together with the biliary ducts and arterial branches. It originates from the pyloric–pancreatic–duodenal veins and penetrates the hepatic parenchyma of segments I and IV. It drains the gastric antrum, duodenum and pancreas.

- (c) Sappey’s aberrant right gastric vein which originates from the gastric antrum, runs within the hepatogastric ligament and enters the hepatic parenchyma at the hilum, anastomosing with the left portal branch, perfusing segments II, III and IV. It drains the stomach and the gastric antrum. In portal hypertension, the reduced portal inflow can cause the compensatory enlargement of this right gastric vein, with reversed flow.
- (d) Paraumbilical veins, which originate in the abdominal wall around the umbilical region, run near the round ligament to drain into the left portal branch. In patients with portal hypertension (PH), these collaterals frequently dilate and become an efferent system with hepatofugal flow.

The blood coming from the third inflow enters the hepatic sinusoids at a different rate as compared to the portal blood flow, thus diluting the portal blood flow after contrast media administration, leading to potential *hypovascular* or *hypervascular pseudolesions*. *Hypovascular pseudolesions* are created by delayed, diluted or missed perfusion. *Hypervascular pseudolesions* are visible during the arterial phase as hyperdense/hyperintense on CT/MRI and as perfusion

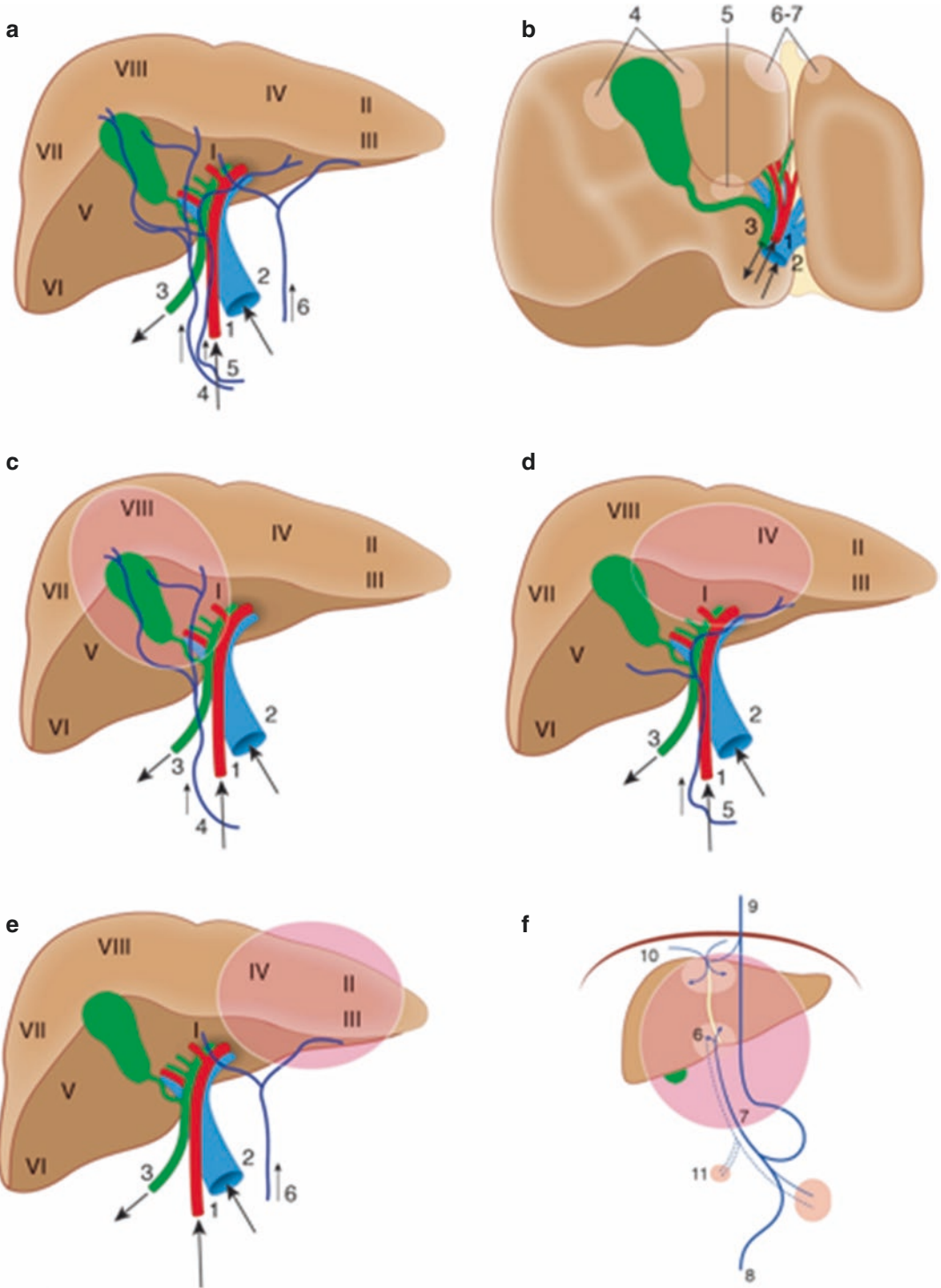


**Fig. 5** Non-portal venous system: Third inflow (a) and liver portions involved in the corresponding perfusion defects (b; view from below). Drawing showing the hepatic segments drained by the cholecystic veins (c), the

parabiliary venous system (Couinaud system) (d), the Sappey's aberrant right gastric vein (e) and the paraumbilical veins (f). Modified from Itai and Matsui 1999; Yoshimitzu et al. 2001; Kobayashi et al. 2010

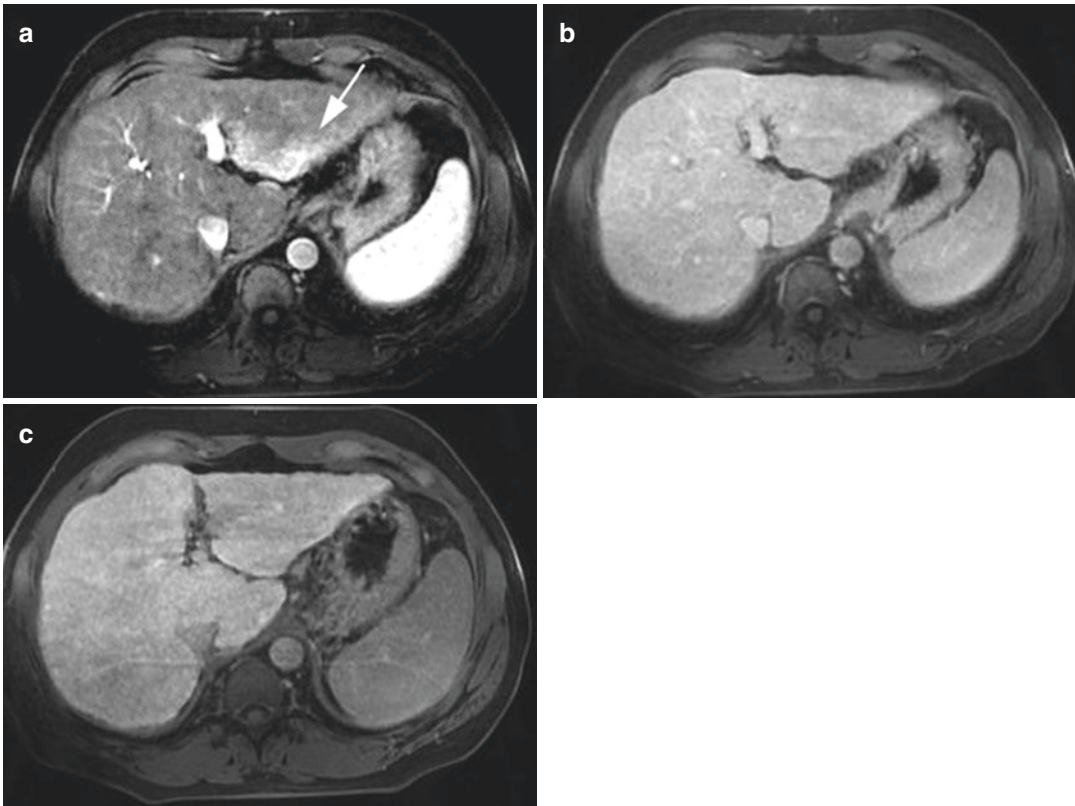


**Fig. 6** THID due to third inflow venous system. Arterial phase image (a) shows a triangular area of enhancement involving the dorsal portion of segment III (arrow) due to

the faster drainage of the Sappey's aberrant right gastric vein. The same area appears isointense in portal (b) and delayed (c) phase images

defects during the portal phase (because the drainage of the third inflow is faster than that of the portal flow) (Fig. 6).

Liver segments I and IV have a higher frequency of portal branch anomalies; during embryogenesis, these two segments have a later portal vein development (32–34th day of pregnancy) than the other segments (26–28th day of pregnancy).

Three main types of hepatic pseudolesions are directly correlated with the non-portal venous system (third inflow): THAD/THID, focal steatosis and focal fat sparing. Each of these hepatic pseudolesions is systematically analysed in the corresponding paragraph.

## 5 Transient Hepatic Attenuation Difference (THAD) and Transient Hepatic Intensity Difference (THID)

Transient hepatic attenuation differences (THADs) are areas of liver parenchymal enhancement during the arterial phase of multiphasic CT of the liver. It is a physiological phenomenon due to the dual supply of the liver, with a localized disparity in hepatic arterial (relatively increased) versus portal venous blood supply (decreased), thus giving a higher attenuation to the affected region. Transient hepatic intensity differences

(THIDs) are the corresponding findings during the arterial phase of dynamic MRI. Therefore, THADs/THIDs derive from regional variations in the portal and arterial supply, due to local *inflow and outflow disorders*.

## 5.1 Hepatic Inflow Disorders

These can be due to: (a) a reduction in portal blood inflow; (b) spontaneous or iatrogenic arterioportal shunts (APSs); (c) an increase in hepatic arterial inflow and (d) outflow reduction.

### 5.1.1 Reduction of Portal Inflow

THIDs/THADs are due to intrinsic portal vein (PV) obstruction from extrinsic hepatic parenchymal compression and/or biliary obstruction.

*Portal vein obstruction* can be due to thrombosis from several causes, such as pylephlebitis, invasion/compression of the portal vein by tumours (HCC or cholangiocarcinoma), infection or surgical ligation. Portal vein obstruction is responsible for a physiological mechanism characterized by a compensatory increase in arterial flow (“arterial buffer response”) (Fig. 7). After a reduction in PV inflow, hepatocytes secrete adenosine and vasopressin mediators which activate the local autonomic nervous system, with consequent vasodilation of the hepatic artery and increased arterial perfusion into the corresponding parenchyma. A 19% reduction in portal inflow induces a vasopressin-mediated increase in arterial flow of about 83%.

Liver parenchymal compression, by the ribs, diaphragm, expansive lesions, perihepatic

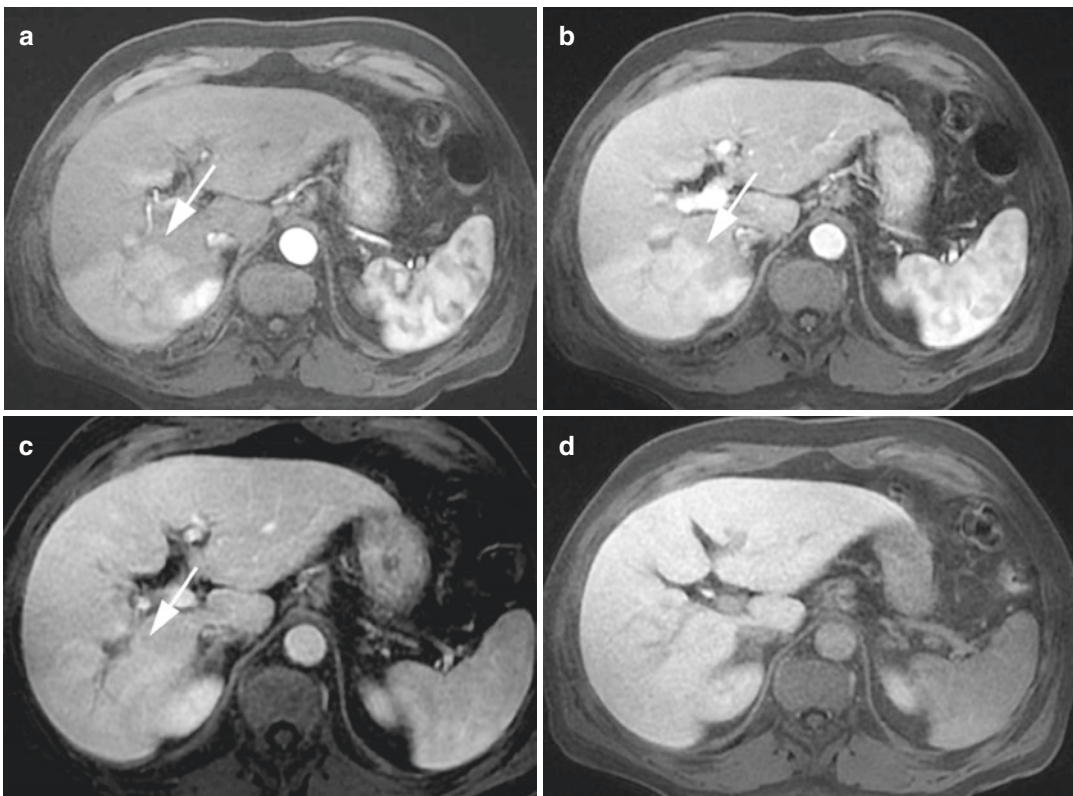


**Fig. 7** Large triangular THID involving the entire segment VII (arrows) due to bland PVT. Arterial phase image (a) showing a large hyperintense wedge-shaped area with persistent enhancement (arrows) during the delayed arterial phase (b) and the portal phase (c) images (arrows).

Delayed phase image (d) demonstrates the recovery of isointensity in the same area as compared to the adjacent parenchyma. Right portal branch thrombosis is evident in the portal phase image (c)

peritoneal collections or pseudomyxoma peritonei, can lead to a regional decrease in portal blood inflow since the portal system is a low-pressure system and is therefore susceptible to extrinsic compression and to local THAD and THID formation. In these cases, THADs/THIDs are reversible and disappear after the resolution of the compressive causes (Yoshimitsu et al. 1999).

Biliary obstruction may also result in decreased portal venous flow by means of obstruction of the peribiliary plexus and can cause THADs or THIDs (Itai and Matsui 1997).

### 5.1.2 Hepatic Arteriportal Shunt (APS) or Iatrogenic Fistula

Hepatic arteriportal shunt (APS) or iatrogenic fistula is the communication between a hepatic arterial branch and the portal venous system resulting in a redistribution of arterial flow in a parenchymal area usually perfused by portal blood flow. Arteriportal shunts can have an iatrogenic origin, occurring after liver biopsies (Fig. 8) or locoregional treatments (percutaneous ethanol injection, thermal ablation and intra-arterial treatments) (Fig. 9) and can also develop

as a consequence of tumours (especially HCC), cirrhosis or trauma.

Arteriportal shunts are usually undetected on grey scale ultrasound (US) but can be diagnosed at Doppler US as a reverse, hepatofugal flow in the portal branch involved parallel to the feeding artery.

Arteriportal shunts can occur through a macroscopic fistula between a large hepatic arterial branch and a large portal branch; they can be detected at contrast-enhanced CT/MRI imaging as the simultaneous opacification of arteries and portal branches during the arterial phase (Itai and Matsui 1997) (Fig. 8).

On dynamic CT/MRI, APSs are typically responsible for areas of parenchymal misperfusion appearing as homogeneously hyperdense/hyperintense during the arterial phase and isodense/isointense during the portal and delayed phases. These areas usually have sharp margins and have no mass effect on the hepatic structures (bile ducts or blood vessels); they are usually stable at imaging follow-up (Galia et al. 2014).

Low flow APSs can show a “dot-like” vascular structure consisting of a portal branch strongly

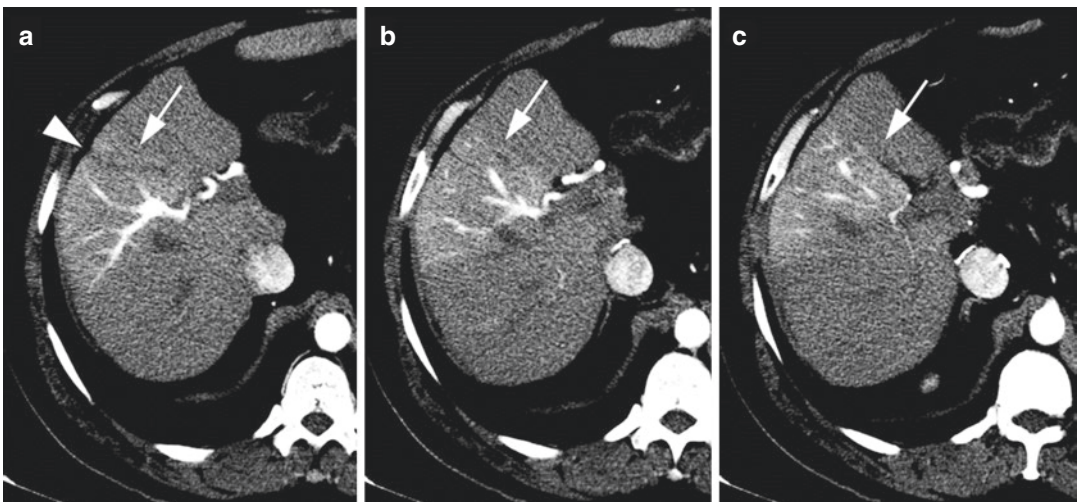


**Fig. 8** Large iatrogenic fistula after liver biopsy and THADs. Arterial phase images (a–c) in different axial planes showing a large hyperenhancing triangular area involving segment V (arrows) with early enhancement of

the corresponding portal branch. This area includes early retrograde enhancement of a large portal branch during the arterial phase of multiphasic CT. Note the hypodense line anterior to the THAD due to the biopsy (arrowhead)

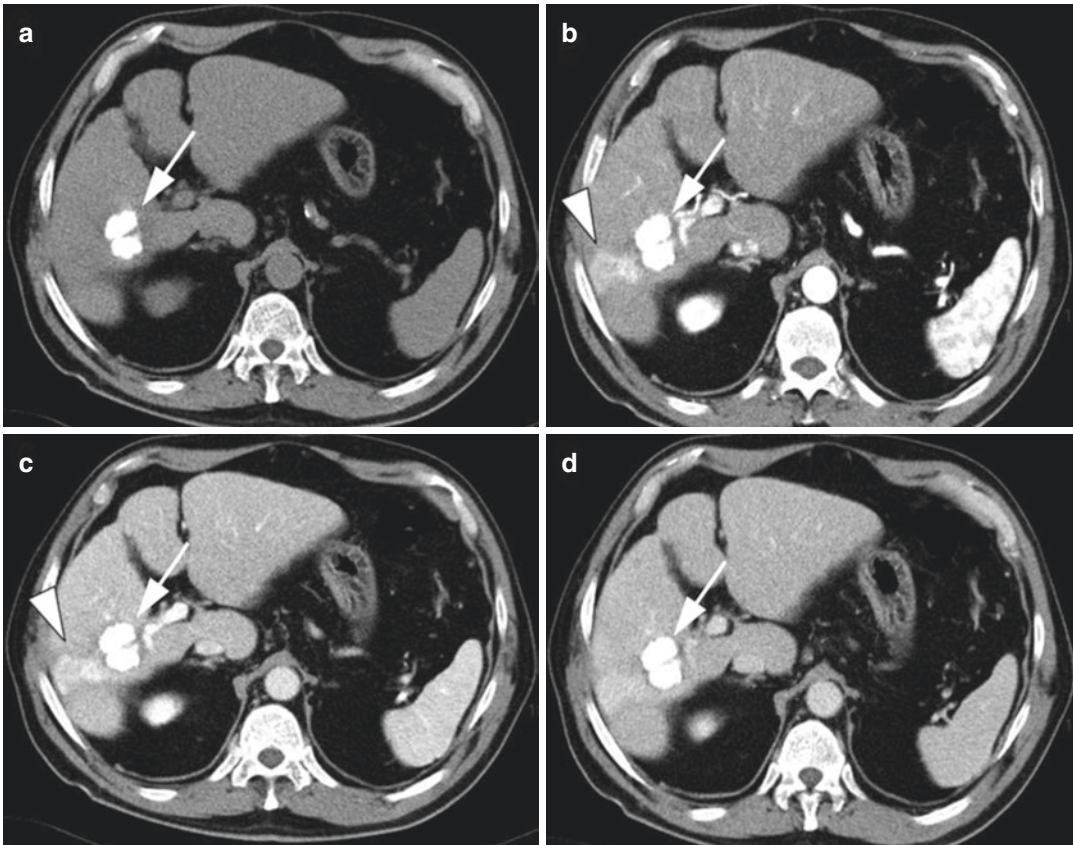


**Fig. 9** THAD following trans-arterial chemoembolization (TACE). Unenhanced-CT image (a) demonstrating round, well-defined lipiodol accumulation in segment VI (arrows) as a result of previous TACE treatment. Arterial phase CT image (b) showing a hypervascular triangular

area (arrowhead) downstream of the lipiodol accumulation, without mass effect and with persistent enhancement (arrowhead) during the portal phase image (c), recovering isodensity on the delayed phase (d)

enhancing during the arterial and venous phase in the middle of a parenchymal triangular-shaped hypervascular pseudolesion (Fig. 10) (Yu et al. 1997). Differentiation from a true malignant liver lesion, such as HCC, relies on the findings of the triangular appearance of the hypervascular area, the “sharp margin sign” and the absence of mass effect.

Depending on the size of an arterioportal fistula, the capacity of the draining portal vein can be worsened by the high-pressure hepatic artery inflow. In small arterioportal shunts, shunted hepatic artery blood joins the adjacent portal vein bloodstream without disturbing flow in the

more proximal portal vein branches (Fig. 11). Conversely, inflow from a large arterioportal fistula can overload the capacity of the intrahepatic portal venous system and precipitate hepatofugal flow in the main portal vein. In the latter case, shunted hepatic artery blood is divided between two routes: (a) the sinusoids, exiting via hepatic veins and (b) the portal vein with reversed flow, reaching the systemic circulation via portosystemic collateral vessels so that the liver is only perfused by arterial blood, and a condition of secondary portal hypertension (PH) can be created (Wachsberg et al. 2002; Bookstein et al. 1982).

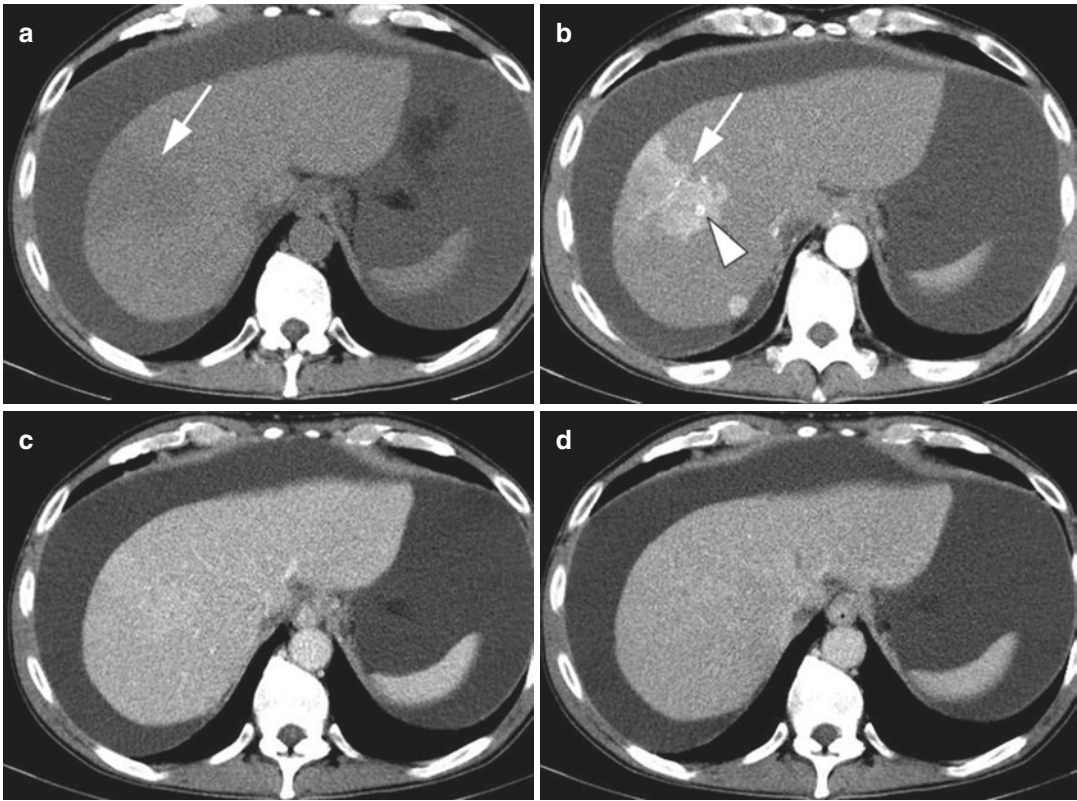


**Fig. 10** Large THAD with the «dot sign». Unenhanced-CT (a) reveals a hypodense trapezoidal area in segment VIII with sharp margins (arrow). The arterial phase (b) shows a hyperattenuation of this area (arrow)

with an internal round, well-defined more hypervascular spot (dot sign) (arrowhead), referring to the early enhancement of a peripheral portal vein. Portal (c) and delayed (d) phases reveal the restored parenchymal attenuation

In the presence of a liver tumour, the morphology of the fistula depends on the site of the tumour in relation to the portal system (Itai and Matsui 1997). When the tumour is located in the apex of the THADs/THIDs, the reduction of the portal flow is caused by portal compression and the THADs/THIDs have a trapezoidal or a fan shape (Fig. 12). When the tumour causes thrombosis of a proximal portal vein, THADs/THIDs are wedge-shaped, and the tumour is located within the perfusion defect (“Shaded area”), and is therefore partially hidden within the perfusion defect in the arterial phase of CT/MRI studies (Fig. 13). Therefore, THADs/THIDs can always be considered as possible sentinel signs of an underlying HCC (Itai and Matsui 1997; Chen et al. 1999a).

An APS can also occur through a trans-vessel shunt from neoplastic thrombus, due to the intra-tumoural neo-angiogenesis of the vasa vasorum, which is responsible for the typical aspect of the “thread and streaks sign” during the arterial phase on contrast-enhanced imaging (Itai and Matsui 1997).

The morphology of THADs/THIDs differs according to the modality of CT/MR reconstructions since, in the axial acquisitions, they can appear as round or oval lesions; therefore, the combined evaluation of 2D and 3D is mandatory (Fig. 14) (Itai and Matsui 1997). The differentiation of a round-shaped enhancing pseudolesion due to THADs/THIDs from hypervascular lesions, such as HCC, in a cirrhotic liver is mandatory. In fact, in cirrhotic

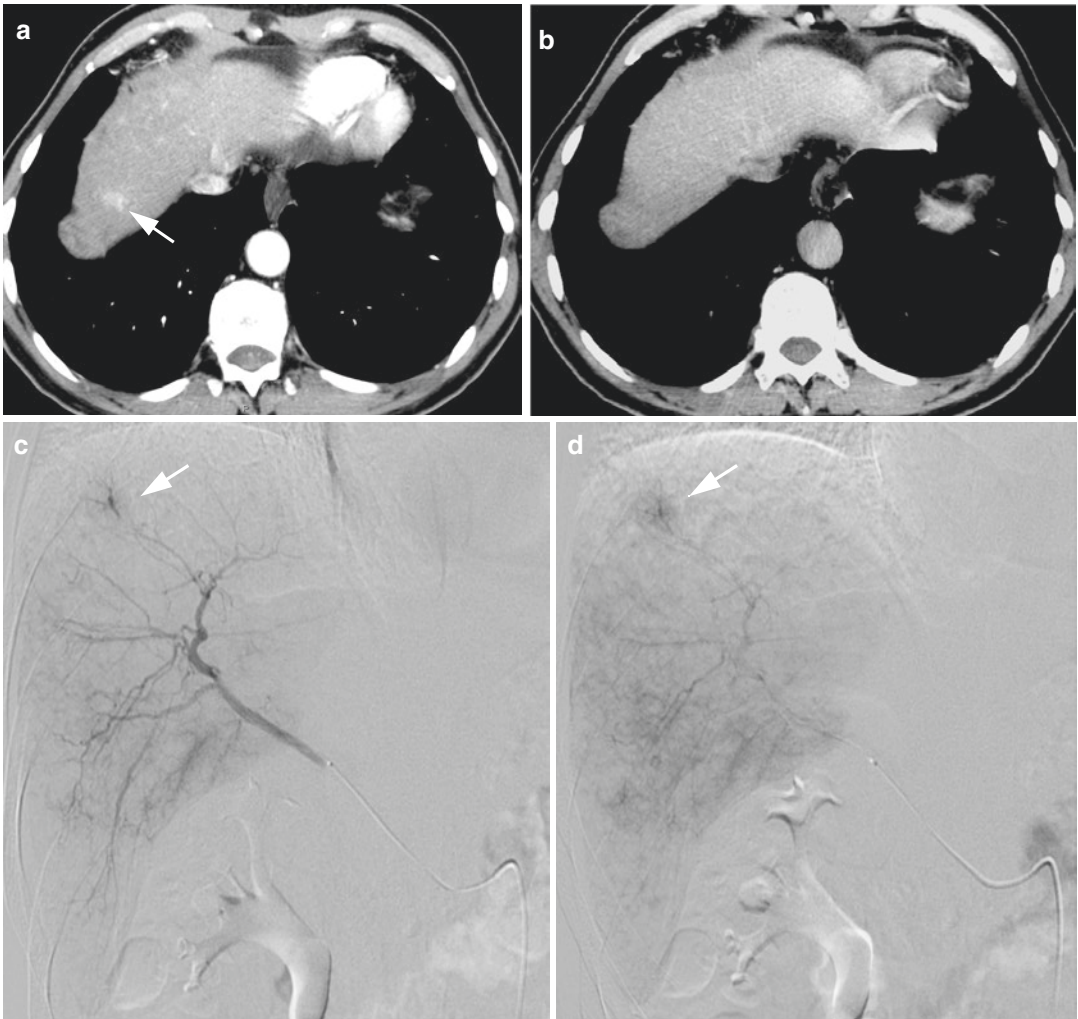


**Fig. 11** Spontaneous arteriportal shunt (APS) in cirrhosis. CT shows a small hyperenhancing area in segment VIII (arrow) during the arterial phase (a), isodense to the adjacent parenchyma in the portal phase (b). The follow-

ing angiography confirms the early enhancement of a peripheral portal branch (arrow) during the arterial phase (c) having a pseudonodular shape (arrow) in the parenchymal phase of the study (d), pathognomonic for APS

patients, a focal hypervascular finding has a 70% probability of being benign and the majority of these are THADs/THIDs due to APSs (Wachsberg et al. 2002; Yu et al. 2000; Shimizu et al. 2003; O'Malley et al. 2005; Kim et al. 2015). The clue to differentiating round-shaped enhancing pseudolesions due to THADs/THIDs from HCC is the absence of wash-out during the portal and delayed phases, without capsule appearance or mass effect on the liver struc-

tures. On MRI, HCC, unlike APSs, is usually slightly hypointense on T1-weighted images and mildly hyperintense on T2-weighted images, round-shaped and it has an evident mass effect on the adjacent liver structures (Vilgrain et al. 2016). Moreover, on MRI performed with HB contrast agents, THADs/THIDs due to APSs appear isointense to the liver parenchyma in the HB phase images, whereas HCC is markedly hypointense (Ronot



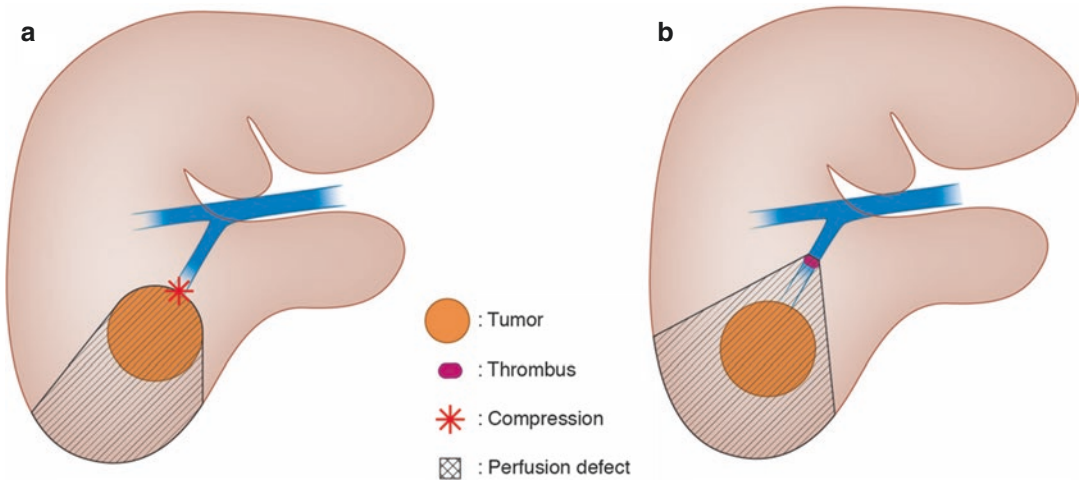


**Fig. 12** Relationship between the morphology of the fistulae caused by a tumour and the site of the tumour in relation to the portal system. Drawing showing a trapezoidal- or fan-shaped THAD/THID when the tumour is

located in the apex (a) or a wedge-shaped THAD/THID when the tumour causes proximal portal thrombosis and is located within the perfusion defect ("shaded area") (b). Modified from Itai Y, Radiology 1997

et al. 2017). In very few cases (5–15%), THADs/THIDs due to APSs appear slightly hypointense on the HB phase of MRI, but the level of SI is always higher than in HCCs (Sun et al. 2010; Motosugi et al. 2010).

Iatrogenic intrahepatic arterial–portal fistula is not a rare complication of liver puncture and transhepatic manipulative procedures, or also after percutaneous ablations or intra-arterial treatments (chemoembolization or radioembolization) of liver tumours (Figs. 8 and 9). It has been reported as a sequela of liver biopsy in about 5% of cases and after transhepatic cholangiography and biliary catheterization in up to 26% of cases (Okuda et al. 1978). However, APSs after biopsy tend to resolve spontaneously. Hellekant et al. reported that the frequency of finding APSs depends on the interval between biopsy and imaging detection; the incidence was as high as 50% in <1 week, dropping to 10% after 1 week (Hellekant 1976). Iatrogenic causes (e.g. percutaneous liver biopsy) represent more than 50% of published cases of APSs (Fig. 8). Similarly, after successful intra-arterial treatment, the necrotic tumoural area can induce direct communication between the arterial and the portal radicles at the

periphery of the treated area, creating an APS (Fig. 9). The majority of APSs resolve spontaneously within a few months as they are small and peripherally located. In rare instances, when APSs are centrally located, clinical symptoms develop (Lee et al. 1997). There have been 30 reported cases of symptomatic intrahepatic APSs following percutaneous liver biopsy. Hepatic arterioportal fistulae can result in portal hypertension secondary to arterial blood flowing directly into the portal vein, bypassing the hepatic sinusoids.

Iatrogenic APS is evident in contrast-enhanced imaging as a peripheral fan-shaped, sharply margined THAD/THID as previously described.

### 5.1.3 Increase in Hepatic Arterial Blood Flow

Increase in hepatic arterial blood flow can be caused by tumour or inflammation. Almost all hepatic tumours, including benign lesions such as hemangiomas, are vascularized by the hepatic artery (both hypervascular and hypovascular tumours). The increase in hepatic arterial flow to the tumour can also lead to an increase in arterial flow to the adjacent parenchyma ("steal

phenomenon”), responsible for THAD/THID appearances (Gryspeerd et al. 1997; Itai et al. 1995; Chen et al. 1999b). The most frequent

inflammatory causes of increase in the hepatic arterial blood flow are cholecystitis or hepatic abscess.

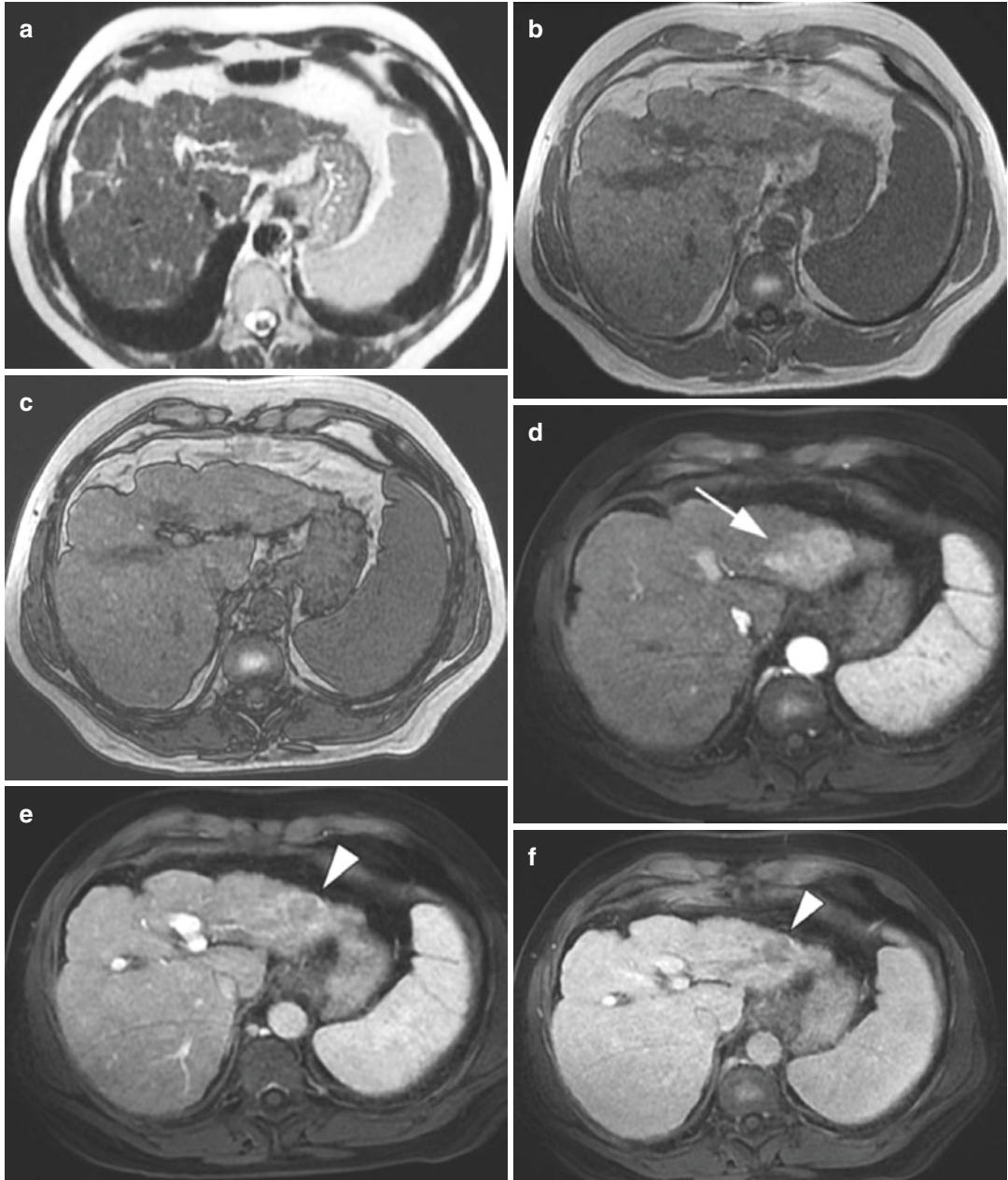


**Fig. 13** THID and “shaded area” on MRI. T2-weighted (a) and T1-weighted “in-phase” (b) and “out-phase” (c) images demonstrating no definite focal lesions. The arterial phase image (d) shows a hyperenhancing wedge-shaped area (arrow), fully involving segment II. Within this area is included a nodular HCC (arrowhead) which is

more evident only due to the washout on the portal and delayed phases (e–f) and due to hypointensity on the hepatobiliary phase image (arrowhead) (g). Diffusion-weighted image (h) reveals restriction (arrowhead) of the nodule

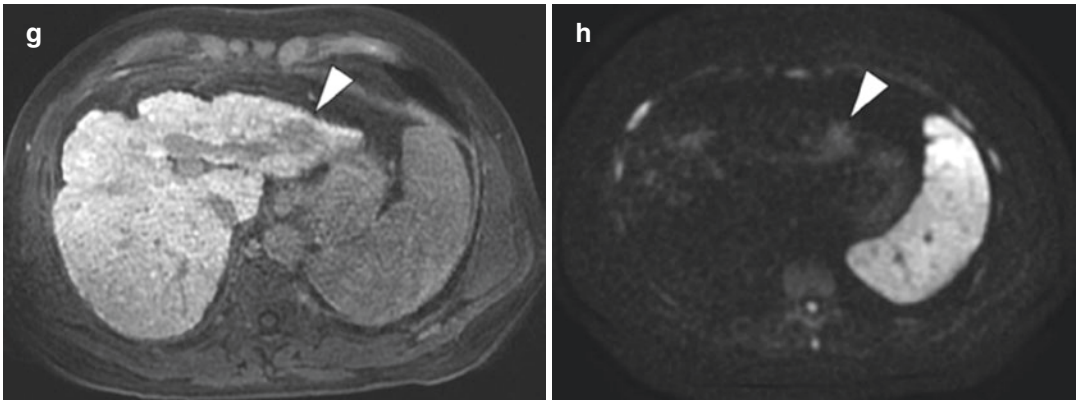
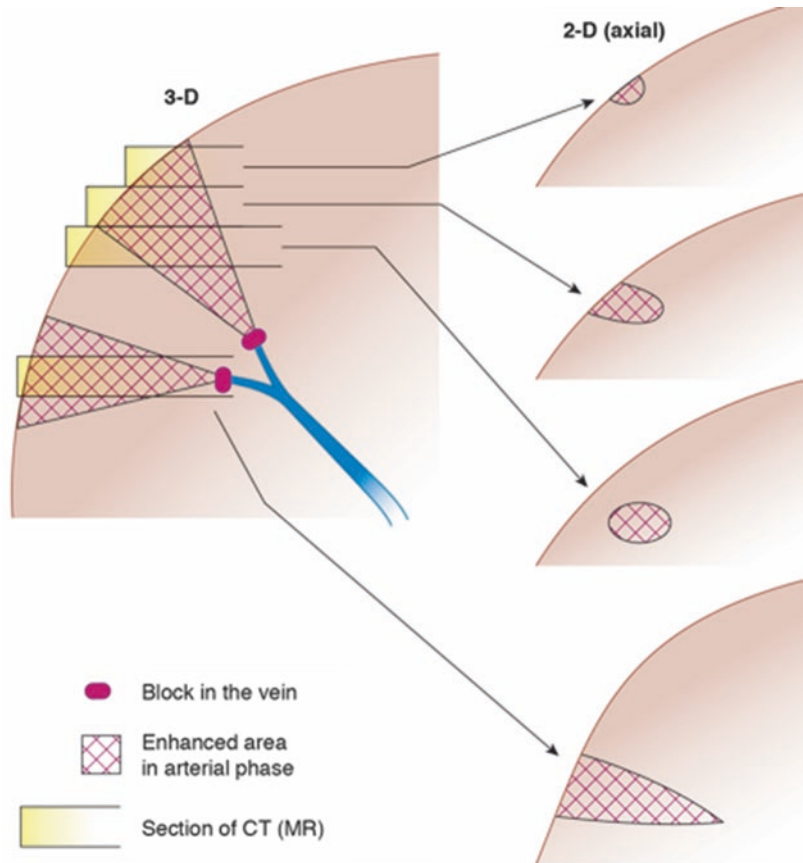


Fig. 13 (continued)

Fig. 14 Relationship between the appearance of a THAD/THID on CT/MRI and the modality of reconstructions: 2D or 3D. Modified from Itai Y, Radiology 1997



### 5.2 Hepatic Outflow Disorders

Outflow disorders inducing a reduction in hepatic vein flow can also be responsible for THIDs/THADs. The increase in sinusoidal pressure due to outflow blockade produces a portal

flow reduction which becomes hepatofugal, and inversion of the pressure gradient between sinusoids and the portal vein system; sinusoidal stasis stimulates adenosine secretion from hepatocytes with subsequent arterial vasodilatation and an increase in the arterial flow (Murata et al.

1995). The main causes of outflow impairment can be functional, such as right heart failure, pulmonary hypertension, pericardial disease and mediastinal fibrosis, or organic, such as Budd–Chiari syndrome and sinusoidal obstruction syndrome (SOS). Complications of Budd–Chiari syndrome and SOS are hepatomegaly, portal hypertension, ascites, jaundice and then cirrhosis (DeLeve et al. 2002).

A pathognomonic CT/MRI pattern of the outflow disorders is heterogeneous enhancement after contrast media administration, with the typical “patchy pattern”, due to hyperdense/hyperintense blood not diluted in the lobules and hypodensity/hypointensity surrounding the portal triad.

Patients with these hemodynamic changes can frequently develop benign LRNs over time (Vilgrain et al. 1999).

## 6 Hemangioma in Cirrhosis

Liver hemangiomas are the most common primary benign liver lesions; they are usually small and are encountered in patients with a normal liver, having an incidence as high as 20% (Karhunen 1986). Hemangiomas are less frequently seen in a cirrhotic background due to the distorted architecture of a fibrotic liver (Brancatelli et al. 2007, 2001; Duran et al. 2015). Some authors have also demonstrated that hemangiomas can become smaller in a liver which is developing cirrhosis (Duran et al. 2015; Mastropasqua et al. 2004). The hallmark of a hemangioma is excessive angiogenesis followed by the regression and inhibition of new blood vessel formation (Makhlouf and Ishak 2002). The diagnosis of a cavernous hemangioma can be obtained on MRI, identifying a very high SI on T2-weighted images (equal to that of gallbladder bile content or cerebrospinal fluid) combined with the typical vascular pattern at dynamic CT/MRI of discontinuous, peripheral, globular enhancement at initial imaging in the arterial phase, with progressive centripetal enhancement

in the portal and delayed phases (Fig. 15) (Brancatelli et al. 2007). In cirrhosis, larger hemangiomas maintain the typical peripheral, discontinuous nodular enhancement pattern and can be diagnosed confidently (Itai et al. 1995). In fact, Mastropasqua et al. (2004) have demonstrated that the hallmarks of hemangiomas did not differ in normal livers as compared to patients with chronic liver disease or cirrhosis. Therefore, the differentiation between hemangiomas and HCC, even in cirrhotic livers is relatively easy since dynamic contrast-enhanced imaging can show the peripheral nodular enhancement, with subsequent central fill-in and sustained enhancement of the delayed phases (Brannigan et al. 2004).

During the follow-up, in cirrhotic livers, hemangiomas can develop scarring, becoming more fibrotic; they usually decrease in size and can be difficult to correctly diagnose at imaging (Brancatelli et al. 2007; Itai et al. 1995).

Therefore, the characterization of a lesion in a cirrhotic liver, such as hemangiomas, should be made with caution and only when classic imaging features are detectable.

### 6.1 Fast-Filling Hemangiomas

An infrequent type of hemangioma is the “fast-filling hemangioma”, also called “capillary” or “flash-filling” hemangioma. On imaging, unlike the cavernous type, it shows complete and homogeneous enhancement during the arterial phase without globular enhancement and without a central fill-in pattern. In these cases, the diagnosis can be uncertain and differentiating them from HCC can be challenging (Jang et al. 2003).

On grey scale US, hemangiomas are hyperechoic but, in rare cases, especially in patients with a fatty liver, they can appear isoechoic, hypoechoic or even with a mixed echogenicity (Yu et al. 2000).

The arterial phase of contrast-enhanced US (CEUS) can be useful in showing the real-time globular enhancement of fast-filling hemangiomas with very rapid central fill-in (Kim et al.

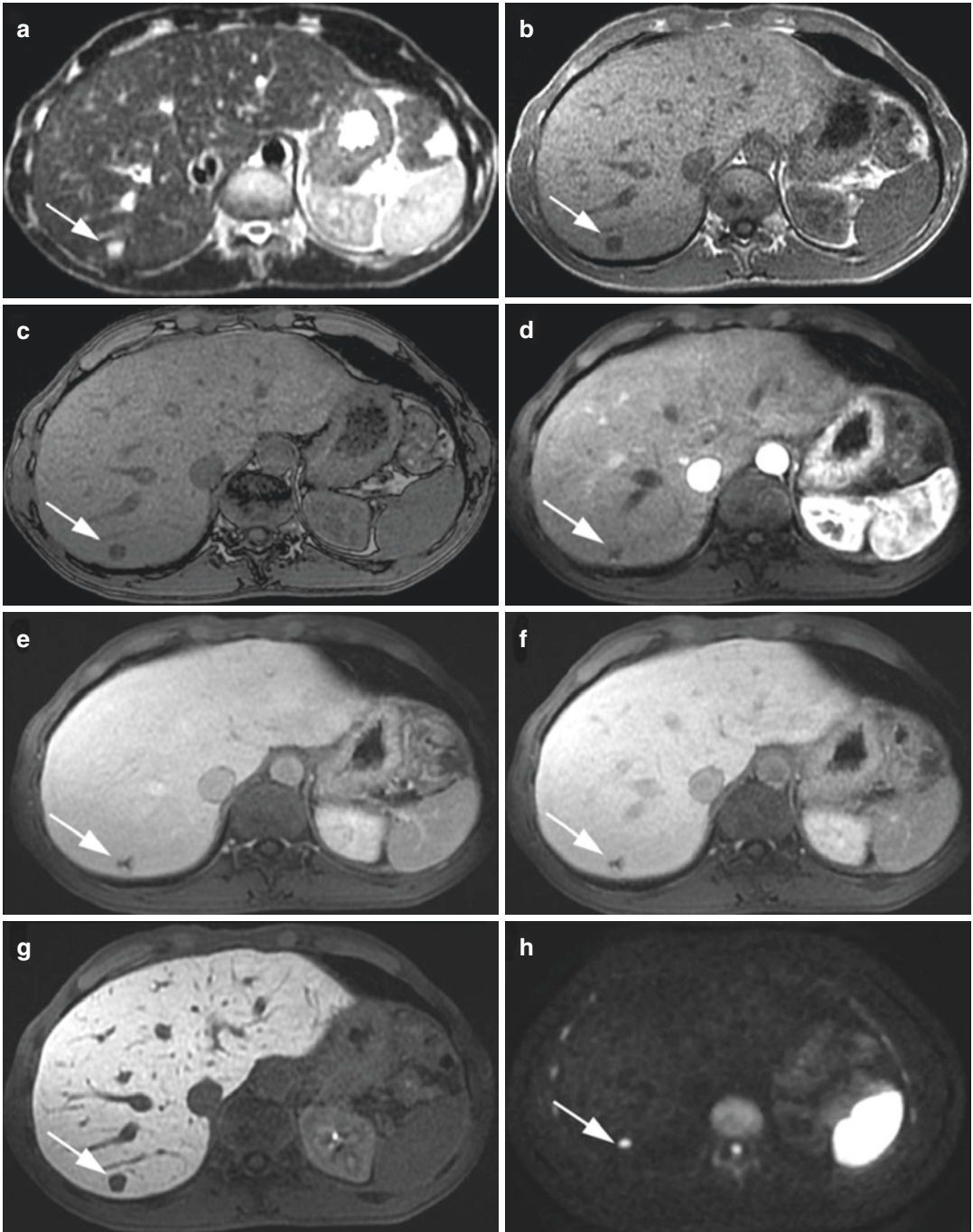


**Fig. 15** Cavernous hemangioma on MRI. T2-weighted image (a) depicts a round strong hyperintense lesion at segment VII (arrow), hypointense on T1-weighted images (arrows) (b, c). Dynamic study after contrast administration shows the typical peripheral and globular enhance-

ment (arrows) (d, e) followed by a central enhancement on the delayed phase (arrow) (f), with hypointensity during the hepatobiliary phase (arrow) (g). Diffusion-weighted image reveals evident diffusion restriction of the lesion (arrow)

2006; Jang et al. 2009a, b; Wilson et al. 2008). However, an important limitation of this technique is that sometimes these pseudolesions can show a mild washout during the portal or delayed phases, caused by microbubble destruction due to continuous ultrasound scanning (Bhayana et al. 2010).

On contrast-enhanced CT/MRI, both fast-filling hemangiomas and small HCCs show hypervascularity in the hepatic arterial phase. However, hemangiomas demonstrate a strong homogeneous enhancement analogous to that of the aorta or other arterial vessels in the arterial phase and similar to the portal vein during the portal phase. Conversely, HCC usually exhibits a milder enhancement during the arterial phase coupled with the typical wash out of contrast media during the portal and delayed phase images (Galia et al. 2014).

On MRI, a typical pattern of all hemangiomas is a strong hyperintensity on T2-weighted images (the “light bulb sign”) useful in the differentiation with HCC, which usually shows only a mild hyperintensity (Tamada et al. 2011).

Therefore, the MRI key findings for the diagnosis of fast-filling hemangiomas are strong hyperintensity on T2-weighted images and enhancement parallel to that of the aorta in the arterial phase, with persistent enhancement in the delayed phase (Fig. 16) (Ronot et al. 2017). Other imaging features can include the presence of hepatic THIDs/THADs at its periphery due to the sump effect (Fig. 17).

Smaller, fast-filling hemangiomas can be difficult to differentiate from small HCC in the HB phase of MRI. (Doo et al. 2009; Goodwin et al. 2011; Francisco et al. 2014; Kim et al. 2016; Dioguardi Burgio et al. 2016) since hemangiomas can exhibit a “pseudo-washout” in the transitional and HB phases (20 min), with the lesion appearing hypointense relative to the surrounding parenchyma due to the rapid uptake of Gd-EOB-DTPA by the background parenchyma (Doo et al. 2009). Radiologists should be aware of this possibility while evaluating patients with

cirrhosis. However, the “pseudo-washout” phenomenon of a hemangioma is more gradual than the true washout in malignant tumours, and attenuation on CT images and SI on MRI typically parallels the enhancement of the blood pool in all phases of contrast enhancement, thus helping in differentiating between hemangiomas and HCC (Kim et al. 2016). The DWI sequences are also of great help; the majority of hemangiomas have the “T2 shine-through effect”, which refers to a high signal on DWI which is not due to restricted diffusion, but rather to a high T2 signal which “shines through” to the DWI. The “T2 shine-through effect” occurs because of the long T2 decay time in some normal tissue. However, Duran et al. have shown that a T2 shine-through effect is less common in flash-filling hemangiomas than in other hemangiomas (Duran et al. 2014).

## 6.2 Sclerosed Hemangiomas

Hemangiomas undergoing degeneration and fibrous replacement are called sclerosed hemangiomas (Brancatelli et al. 2009). Several imaging findings of sclerosed hemangiomas have been described in different series, such as the lack of early enhancement, gradual and persistent mild peripheral enhancement (Doo et al. 2009; Kim et al. 2016; Brancatelli et al. 2009; Itai and Saida 2002) and mild hyperintensity on T2-weighted images, much lower than typical hemangiomas (Brancatelli et al. 2009). Other imaging features include geographic margins, capsular retraction, decrease in size over time, presence of hepatic THIDs/THADs at their periphery and loss of previously seen regions of enhancement at follow-up (Goodwin et al. 2011). However, these imaging findings are non-specific and, therefore, correct differentiation from malignant tumours is difficult (Itai and Saida 2002); in the majority of cases, sclerosed hemangiomas are diagnosed only by pathologists after biopsy or surgical excision.

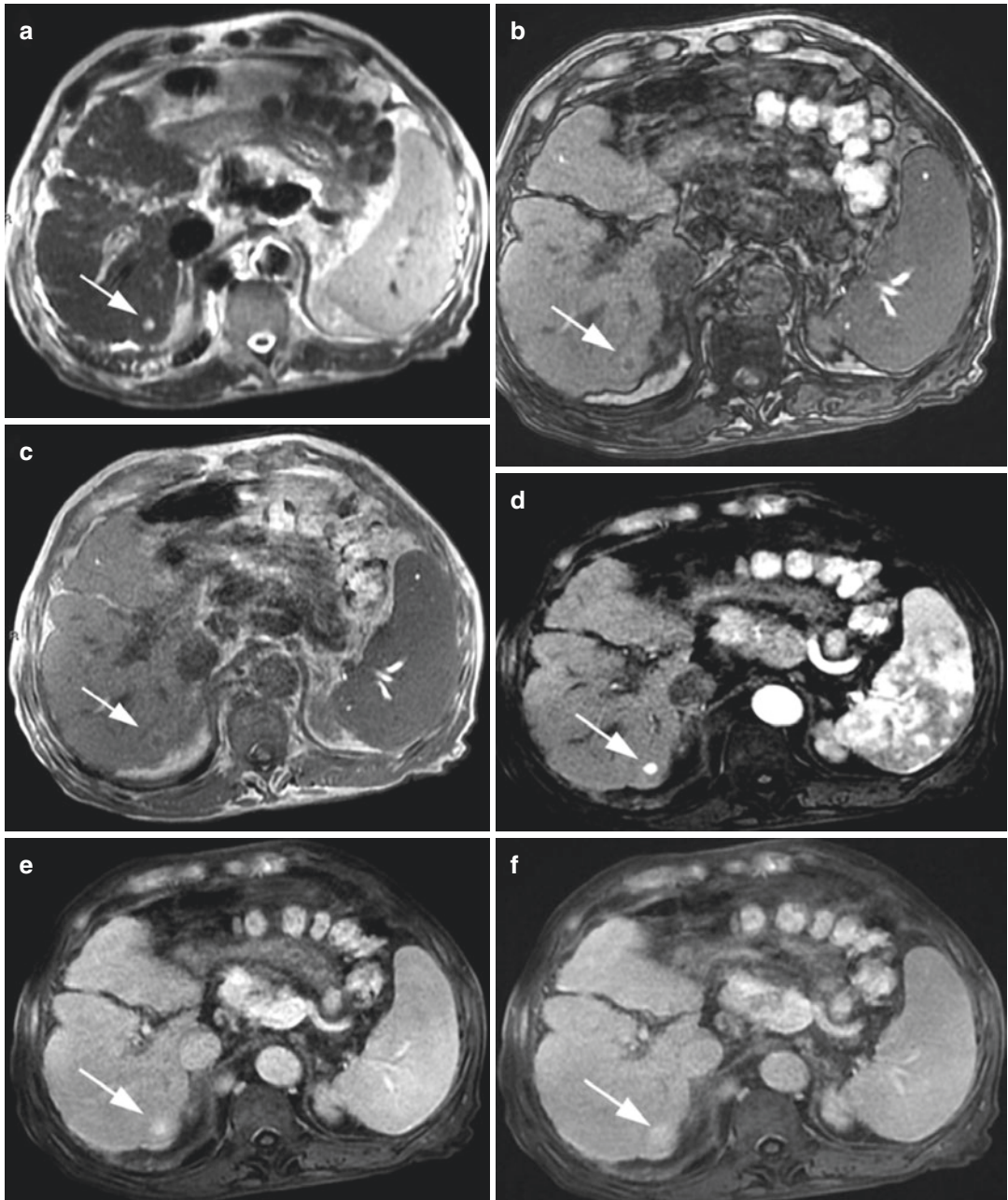


**Fig. 16** Fast-filling hemangioma on MRI. T2-weighted image (a) depicts a small strong hyperintense lesion at segment VI (arrow), hypointense on T1-weighted images (arrows) (b, c). Dynamic study after contrast administration shows complete and rapid filling-in (arrow) during

the arterial phase (d), persisting during the portal and delayed phases (arrows in e, f) and hypointensity on the hepatobiliary phase (arrow) (g). Diffusion-weighted image (h) confirms evident diffusion restriction of the lesion (arrow)

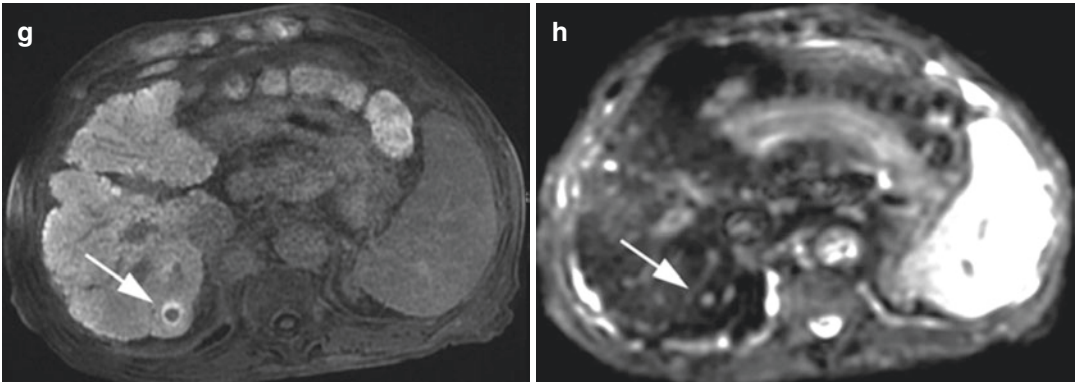


**Fig. 16** (continued)

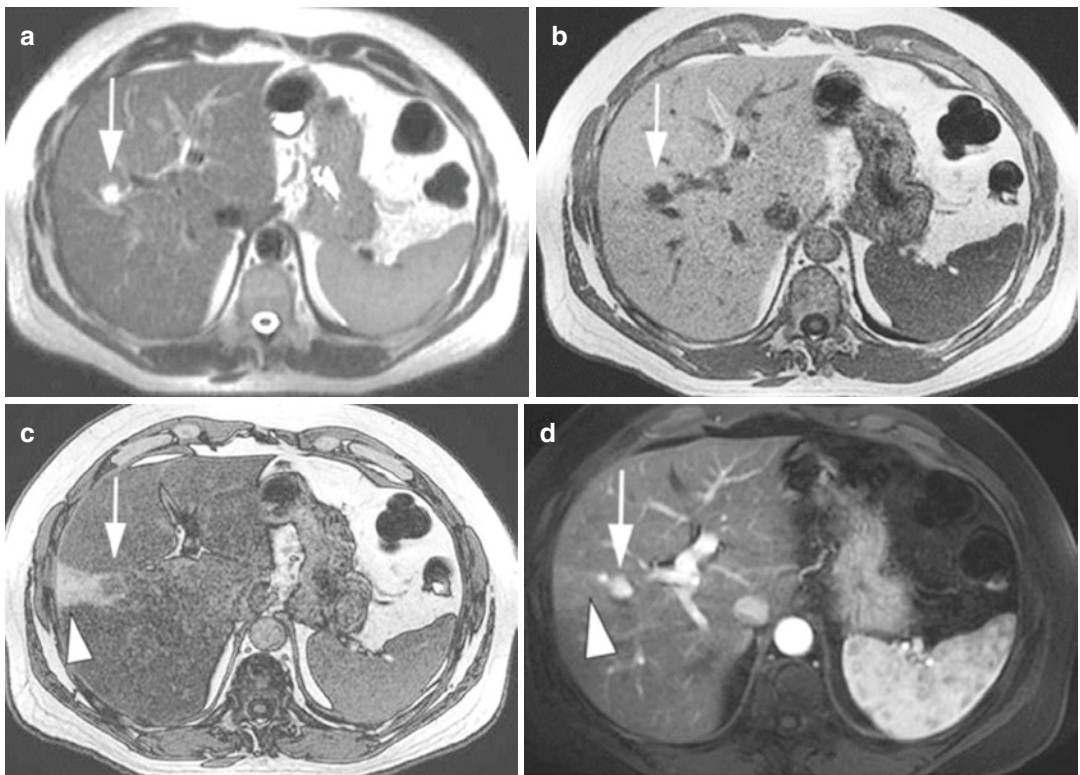


**Fig. 17** Fast-filling (or capillary) hemangioma with peripheral THID and focal fat sparing area on MRI. T2-weighted image (a) shows a small strong hyperintense lesion in segment VIII (arrow), hypointense on T1-weighted images (arrows) (b, c), on the apex of a wedge-shaped area (arrowhead) hyperintense on the T1-weighted “out-of-phase” image (c) as compared to adjacent hypointense steatotic parenchyma, appearing isointense on the T1-weighted “in phase” image (b), characteristic of a hemangioma with a peripheral focal fat-

sparing area. The dynamic study after contrast administration shows complete and rapid filling-in of the hemangioma (arrows) and hyperintensity of the peripheral THID (arrowhead) during the arterial phase (d), persisting during the portal and delayed phases (arrowheads) (e, f) with hypointensity of the hemangioma (arrow) on the hepatobiliary phase (g). Diffusion-weighted image (h) reveals strong diffusion restriction of the hemangioma (arrow)



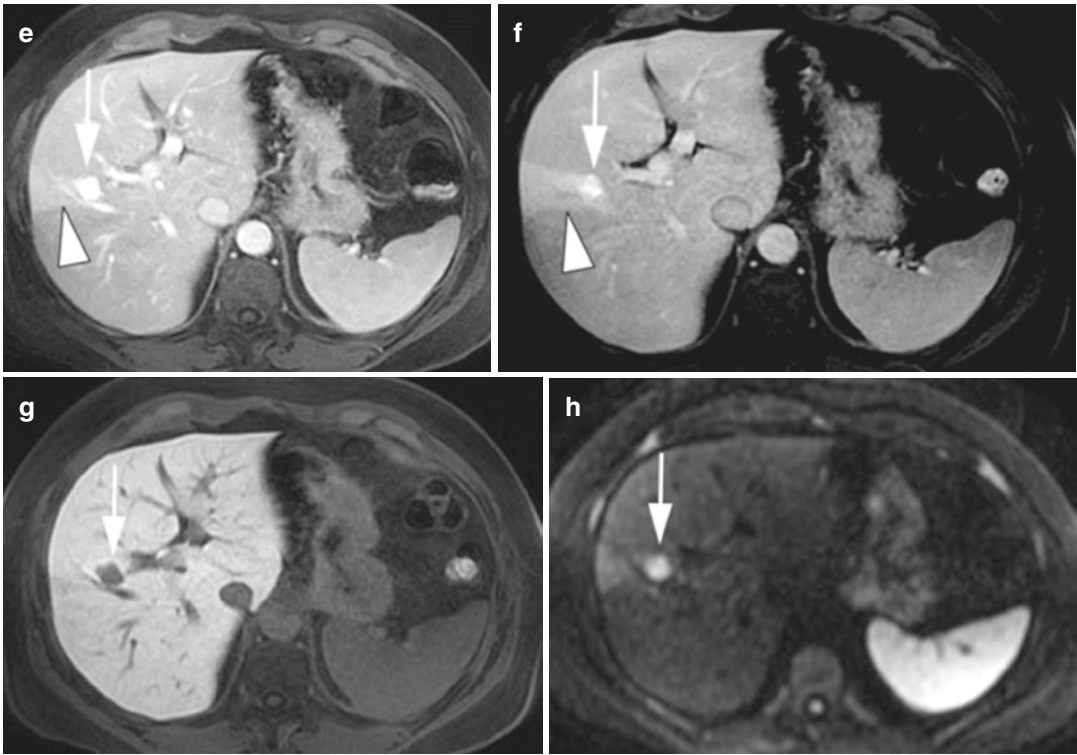


**Fig. 17** (continued)

## 7 Pseudomass in Cirrhosis and Chronic Portal Vein Thrombosis (PVT)

When the main portal vein is obstructed by thrombosis, many collaterals are gradually hypertrophied in order to provide a compensatory liver inflow, forming the “cavernous transformation of the portal vein”, also called “portal cavernoma” (Chen et al. 2017). In the case of PVT, the “central zone” of the liver parenchyma, close to the hepatic hilum, preferentially receives the residual portal venous flow by collaterals (via the parabiliary venous system, peribiliary plexus and proximal accessory branches of the main portal vein) as compared to the peripheral liver which is perfused to a lesser degree from a predominantly arterial supply, which is thought to occur via trans-sinusoidal arterioportal shunts (“zonal perfusion” theory). The central zone, including the

caudate lobe and perihilar hepatic parenchyma gradually becomes relatively hypertrophic and may simulate a mass-like lesion. Conversely, the peripheral zone of the liver gradually becomes atrophic, despite the arterial compensation. The concept of “central” and “peripheral” zones may also be of value in explaining the deformity of a cirrhotic liver with portal hypertension since PH may induce hemodynamic changes of portal flow similar to those seen in portal cavernomas (Itai et al. 1994).

These hemodynamic and morphologic changes in chronic PVT determine the following typical appearances on contrast-enhanced CT-MRI imaging; the atrophic peripheral region of the liver shows hyperenhancement in the arterial phase, whereas the enlarged central zone displays hypoenhancement, mimicking a large mass. In the delayed phase, the central zone shows isoenhancement to the liver (Chen et al.

2017) helping in the differential diagnosis with true lesions. Magnetic resonance imaging with hepatospecific contrast media can help in the differential diagnosis of pseudomass in chronic PVT which is isointense to the surrounding liver in the HB phase as compared to true lesions, usually hypointense (Fig. 18).

---

## 8 Confluent Fibrosis

In cirrhotic livers, fibrosis can be diffusely or heterogeneously distributed (Galia et al. 2014). In some cases, fibrosis can become focal and confluent due to the coalescence of fibrous tissue, with consequent development of large fibrous scars (Ohtomo et al. 1993a, b). Confluent fibrosis is more frequent in alcoholic cirrhosis and less frequent in other etiologies, such as primary sclerosing cholangitis or autoimmune chronic hepatitis (Vilgrain et al. 2016).

Focal fibrosis is typically wedge-shaped, with the base on the subcapsular region, radiating from the porta hepatis, frequently involving segments IV, VII or VIII, and associated with capsular retraction or focal flattening (retraction) of the hepatic capsule (Ohtomo et al. 1993a, b) (Fig. 19). In approximately 15% of cases, the hepatic vessels can become part of (“trapped”) the focal fibrosis, appearing irregular but patent (Brancatelli et al. 2009). The typical peripheral location of fibrosis can be explained by the zonal perfusion changes occurring in cirrhosis, as previously described (Breen et al. 2004).

Ultrasound is widely used as a first-line imaging modality in the evaluation of patients with cirrhosis. However, measurements of liver echogenicity have shown poor accuracy in diagnosing fibrosis (Mathiesen et al. 2002).

On CT, fibrosis appears as a wedge-shaped region of hypoattenuation on unenhanced images, persisting on the arterial and portal venous phases which may gradually enhance in the delayed phase. This feature is explained by the slow contrast accumulation in the extracellular compartment characteristic of the fibrous tissue (Décarie et al. 2011).

On MRI, fibrotic septa in cirrhotic livers include reticulations surrounding regenerative nodules leading to the typical “lace-lake pattern”. These fibrous septa are hypointense on T1-weighted images and hyperintense on T2-weighted images and enhance at the equilibrium phase after gadolinium administration. Usually, on contrast-enhanced MRI with extracellular agents, unlike HCC, focal fibrosis does not enhance during the arterial phase but can slightly enhance during the portal phase and highly enhance during the delayed phase (Fig. 19) (Vilgrain et al. 2016).

In rare cases, focal confluent fibrosis can mimic the appearance of an infiltrative HCC (Ohtomo et al. 1993a, b) when it shows irregular margins and mild enhancement on the arterial phase of contrast-enhanced imaging. Enhancement during the arterial phase could be explained by the associated inflammation (Goodwin et al. 2011), especially in the early phase of its development in which confluent fibrosis might not be associated with capsular retraction (Fig. 20) (Galia et al. 2014; Francisco et al. 2014). However, progressive enhancement from the arterial to the delayed phases helps in differentiating focal confluent fibrosis from infiltrative HCC, which shows the typical washout pattern (Ohtomo et al. 1993a, b). Magnetic resonance imaging with HB agents is less useful than MRI with extracellular contrast media in the differential diagnosis of focal confluent fibrosis and infiltrative HCC since, during the transitional (at about 5 min from contrast media injection) and the HB (at about 20 min) phases, both focal confluent fibrosis and HCC are typically hypointense, the first due to the lack of hepatocytes and the second due to degenerated hepatocytes. Other MRI features could be helpful in differentiating confluent fibrosis from HCC: mild hyperintensity on T2-weighted images, although some HCCs can show the same feature (Ohtomo et al. 1993a, b), and a diffusion restriction in DWI, but with an apparent diffusion coefficient (ADC) slightly higher than that of HCC (Park et al. 2013).

Other imaging characteristics pointing towards infiltrating HCC are contour bulging, satellite nodules and neoplastic PVT (Dioguardi

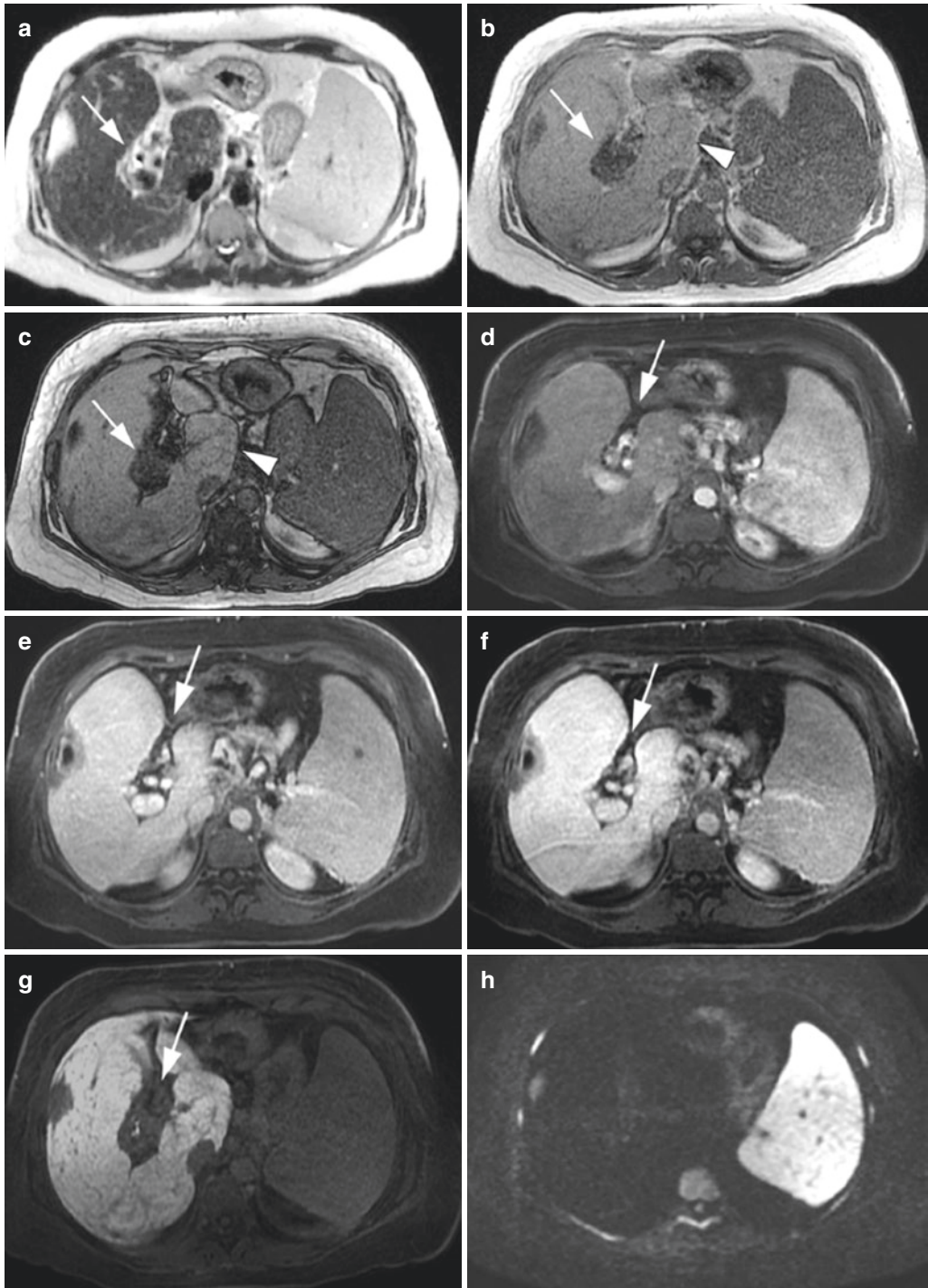


**Fig. 18** Liver pseudomass in the presence of portal cavernoma on MRI. T2- and T1-weighted images demonstrating a pseudomass at the hepatic hilum (arrows), hyperintense on the T2-weighted image (a) and hypointense on T1-weighted images (b, c) with hypertrophy of segment I (arrowheads). The arterial (d), portal (e) and

delayed (f) phases confirm the presence of multiple dilated vessels at the hepatic hilum (cavernous transformation of the portal vein (arrows)). Hepatobiliary phase (g) revealing hypointensity of the pseudomass at the hepatic hilum (arrow) with no restriction on the diffusion-weighted image (h)

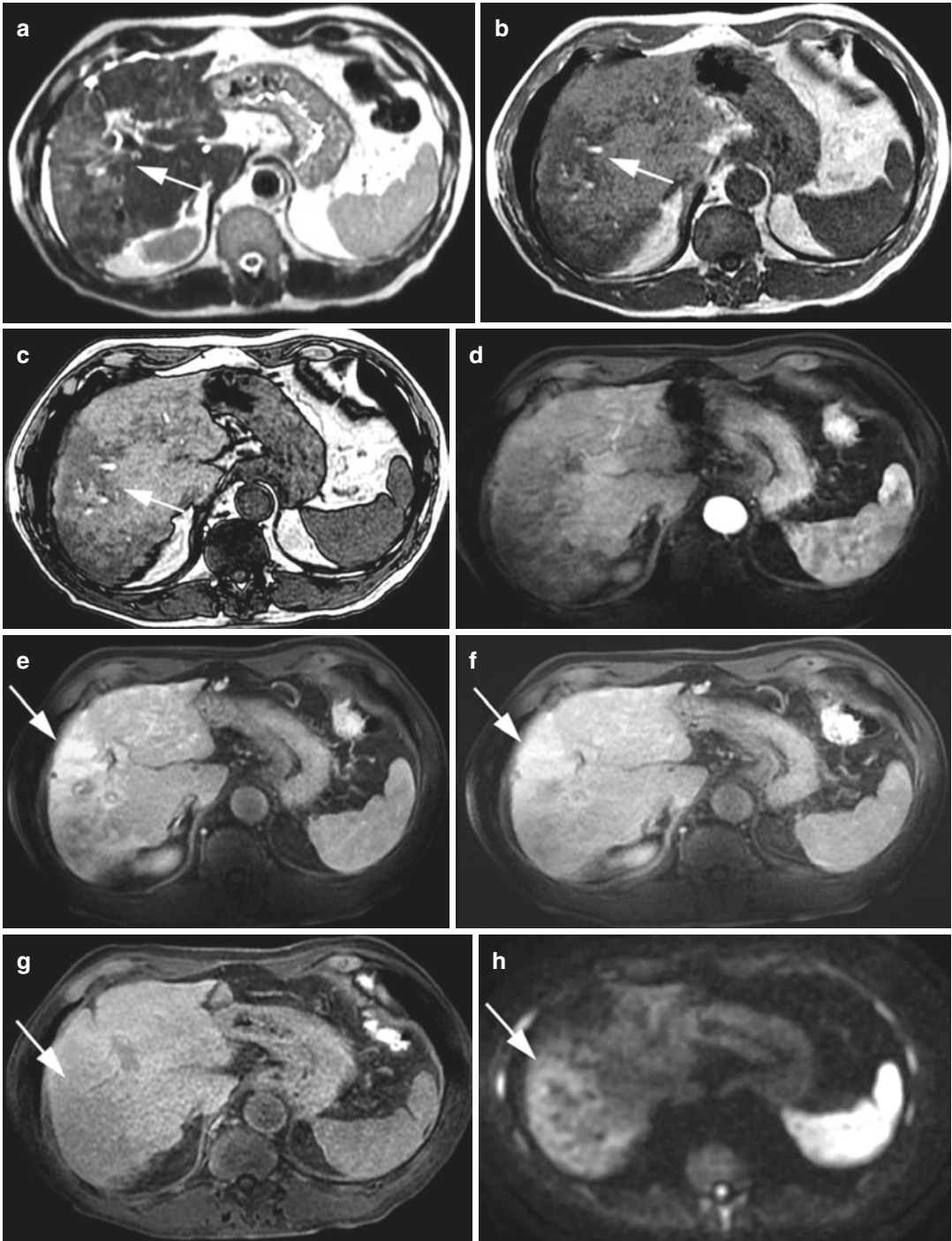


**Fig. 19** Confluent fibrosis on MRI. T2-weighted image (a) shows an irregular peripheral hyperintense area (arrow) involving segments V and VI, hypointense on T1-weighted images (b, c, arrows). Arterial phase (d) showing no significant enhancement of this area, distorted

vessels at its periphery, and late enhancement (arrows) in the portal-venous (e) and delayed (f) phases coupled with hypointensity (arrow) on the hepatobiliary phase (g). A typical mild restriction (arrow) of the entire area is shown in the diffusion-weighted image (h)

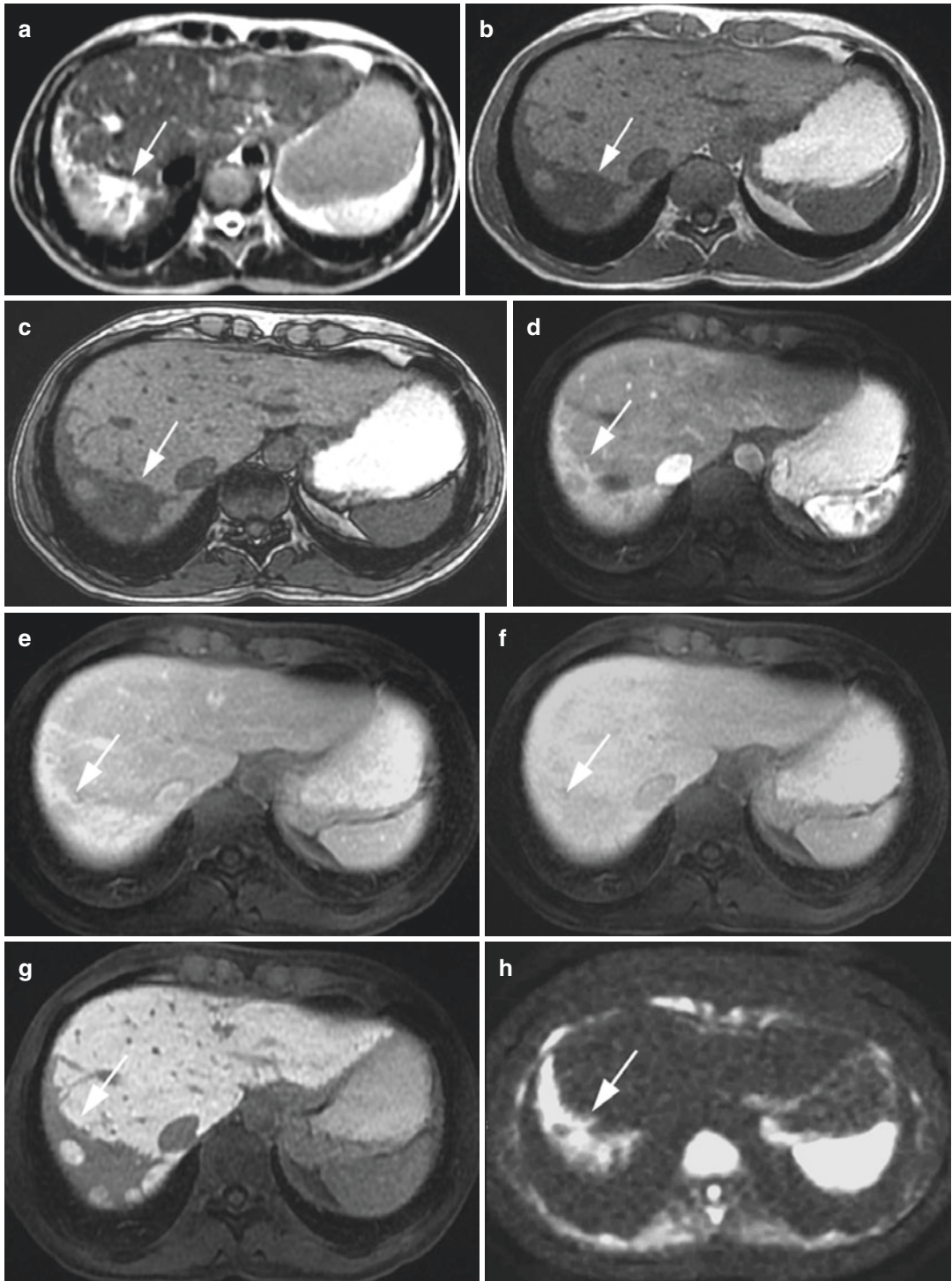


**Fig. 20** Confluent fibrosis on MRI. T2-weighted images (a) demonstrating an irregular strongly hyperintense area largely involving segment VII (arrows), hypointense on T1-weighted images (b, c, arrows). The dynamic study shows hyperintensity of this area (arrows) during the arterial (d) and portal (e) phases, with isointensity (arrow) in the delayed (f) phase and hypointensity (arrow) during the hepatobiliary (g) phase. Diffusion-weighted image (h) reveals a strong diffusion restriction (arrow)

Burgio et al. 2016; Park et al. 2013), all absent in focal confluent fibrosis.

In the absence of these key features for differentiating confluent fibrosis from HCC and when the differential diagnosis remains uncertain, image-guided biopsy is mandatory (Vilgrain et al. 2016).

## 9 Focal Fatty Changes

Fatty liver disease is a pathological condition in which triglycerides accumulate within the cytoplasm of hepatocytes, due to an altered hepatocellular lipid metabolism and a defect in free fatty acid metabolic pathways (Brunt and Tiniakos 2002; Angulo 2002). Fatty liver disease usually does not get worse but, in the final evolution, it can cause scarring of the liver, which leads to cirrhosis.

Two main conditions are responsible for this aberrant fat accumulation: alcoholic liver disease and non-alcoholic fatty liver disease (NAFLD) related to insulin resistance and metabolic syndrome. Other less common causes of fat accumulation are viral hepatitis, drug overuse, dietary and nutritional abnormalities and congenital disorders.

Typically, lipid accumulation affects the centre of the hepatic lobule, near the central vein, and subsequently involves the peripheral zone, near the portal triads (Brunt and Tiniakos 2002) whereas, in advanced steatosis, the lipid accumulation involves the entire hepatic parenchyma (Scheuer and Lefkowitz 2000), frequently with inhomogeneous distribution, resulting in the formation of fat sparing areas (i.e. around the gallbladder, hepatic hilum, posterior edge of segment IV) (Matsui et al. 1995).

*Fat-sparing areas* in diffuse steatosis involve the same regions affected by *focal fat accumulation*: most frequently the perivascular and subcapsular regions, hepatic hilum and along the insertion of the falciform ligament (Hamer et al. 2006; Mathieu et al. 2001). This is explained by the different blood supply of these regions where portal flow is replaced by the third inflow (see corresponding paragraph) (Itai and Matsui 1999).

The third inflow causes local hemodynamic anomalies which produce focal tissue hypoxia; the high insulin content in the parabiliary venous system and right gastric vein predispose to the accumulation of fat into hepatocytes in the territories perfused by these aberrant veins (Fig. 21).

*Focal fatty deposition* is often a simple diagnosis, due to some key imaging features, such as fat content in characteristic areas, absence of mass effect on adjacent structures of the liver, contrast enhancement similar to those of the hepatic parenchyma, irregular margins and geographic rather than a round-shaped configuration. Fat sparing or local fat depositions are small areas which are rarely confluent (Angulo 2002).

*On US, fat-sparing areas* are usually homogeneous hypoechoic zones within a bright liver background and colour Doppler can reveal a hepatopetal flow in the lesion. Contrast-enhanced ultrasound is helpful in confirming the benignity of these findings, showing normal arterial and portal perfusion in the surrounding parenchyma (Nicolau and Brú 2004) and an early opacification of small venous branches within the lesion, during the arterial phase, caused by aberrant splanchnic venous drainage. However, *focal fat depositions* are homogeneously hyperechoic on US, with normal arterial and portal perfusion as compared to the adjacent liver parenchyma on CEUS, as in fat-sparing areas.

*On unenhanced CT*, the diagnosis of a fatty liver is based on a liver density lower than 40 Hounsfield units (HU) (Boyce et al. 2010) or an attenuation difference higher than 10 HU between the spleen and the liver (Alpern et al. 1986). Liver parenchyma hypoattenuation relative to the liver vasculature establishes the presence of moderate to severe fatty liver disease (Hamer et al. 2006). On portal phase contrast-enhanced CT, an attenuation difference greater than 25 HU between the spleen and the liver suggests fatty liver deposition (Fig. 22) (Alpern et al. 1986). However, *focal fat sparing* appears as a hyperdense area in a steatotic background, but with normal HU and with absent mass-effect on the adjacent vessels.

*On MRI, focal fat sparing areas* appear isointense to the liver parenchyma on “in-phase” T1-weighted images and hyperintense on

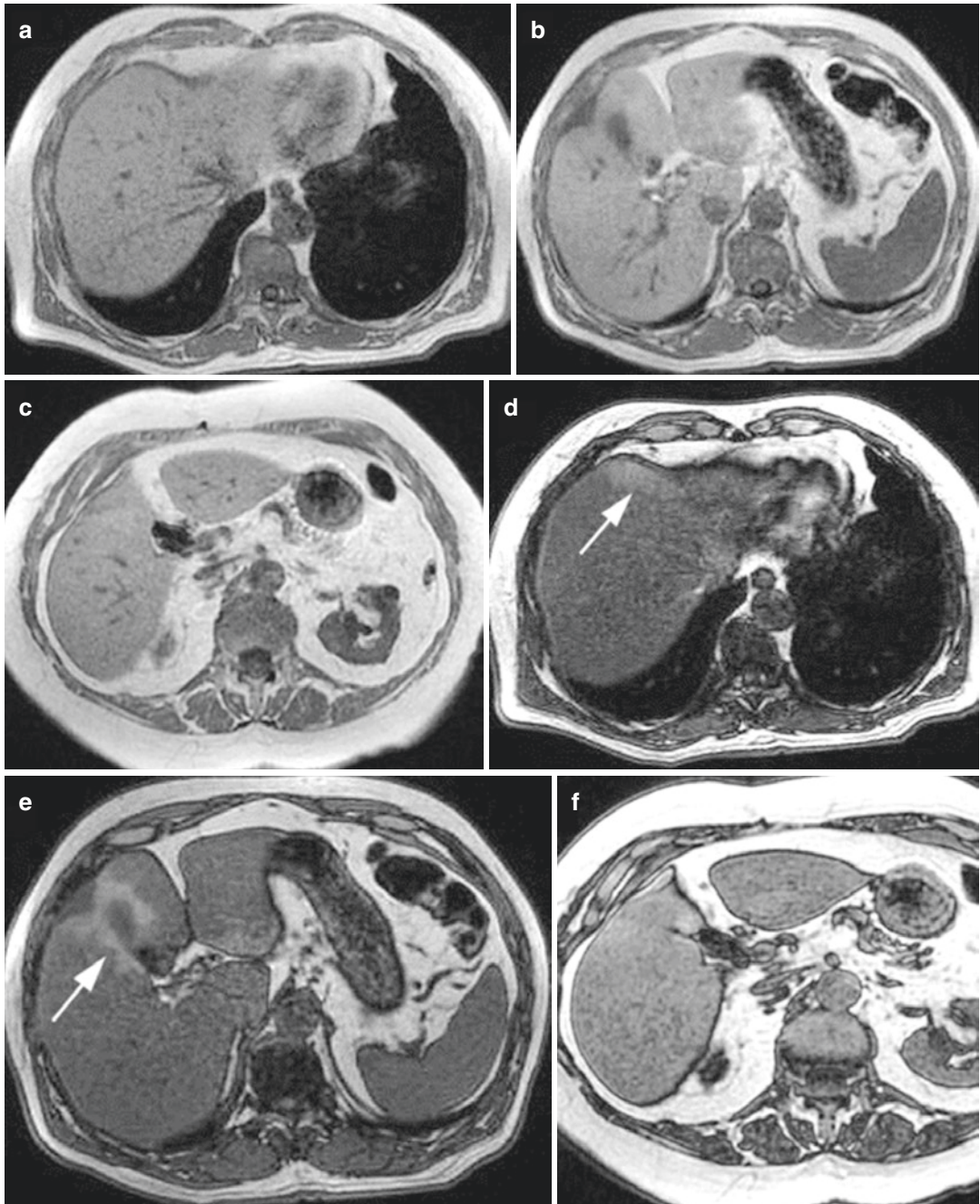


**Fig. 21** Focal fat-sparing area on MRI. T1-weighted “in-phase” (a–c) and “out-phase” (d–f) images in different planes. In T1-weighted “out-of-phase” images (d–f), a hepatic dropout of signal intensity of the entire liver with

a focal hyperintense area (arrows) in segments VIII, V and IV, characteristic of a focal fat sparing area adjacent to the gallbladder

“out-phase” T1-weighted images (Fig. 23). Nevertheless, *focal fat depositions* on T1-weighted images show a significant loss of SI

on “out-phase” as compared to “in-phase” images, due to chemical shift artefacts (Hamer et al. 2006). Moreover, focal fat accumulation is

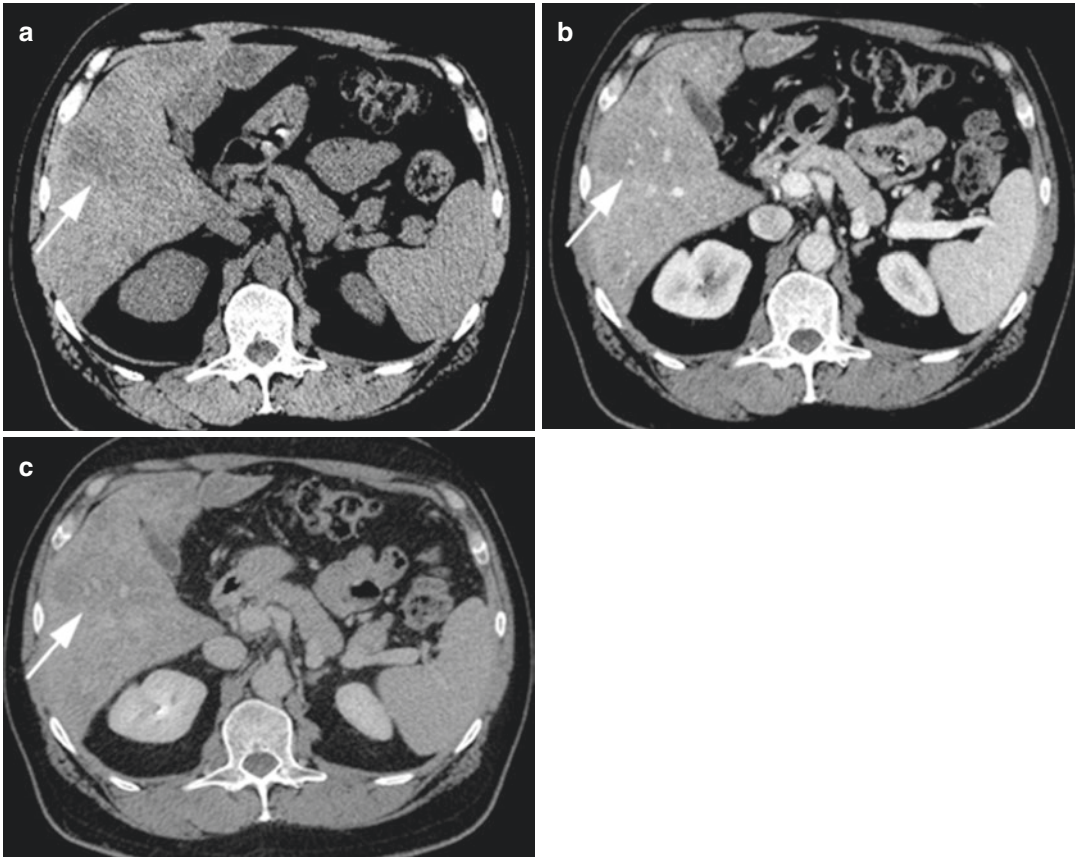


**Fig. 22** Geographic steatosis on CT. Unenhanced CT (a) revealing geographic hypodense areas involving segments V, IV and III (arrow), with persistent mild hypodensity

(arrows) during the portal (b) and delayed (c) phases, characteristic of geographic steatosis

not hyperintense on DWI, thus confirming its benignity (Fig. 24).

A rare pattern of fatty deposition is that, in the perivascular areas, surrounding vessels, such as portal vein branches or central hepatic venules, appear as tram-like or ring-like fatty lesions, depending on imaging plans. Ring-like fatty deposition can mimic metastases or HCC (Hamer et al. 2006). A diagnosis regarding the evaluation of T1-weighted “in-phase” and “out-phase” images can easily be achieved.

Another pattern is the subcapsular fat deposition which may appear as a confluent fat area confined in the peripheral zone or sometimes appearing as small fatty nodules (Hamer et al. 2006). The subcapsular pattern may be idiopathic or may be related to the use of insulin added to the peritoneal dialysate in patients with insulin-

dependent diabetes and renal failure (Sohn et al. 2001; Khalili et al. 2003). In these patients, insulin promotes the esterification of free fatty acids into triglycerides, especially in subcapsular hepatocytes, because they are exposed to a higher insulin concentration. A patient’s clinical history should be helpful in achieving a correct diagnosis.

The last rare pattern of fat deposition is multifocal fat infiltration, also known as “multinodular hepatic steatosis” (Prasad et al. 2005). Round foci of fat deposition are disseminated within the liver, also in atypical regions, mimicking true hepatic nodules (Kroncke et al. 2000; Kemper et al. 2002). A differential diagnosis can be challenging in cases of a patient with a known history of malignancy. Moreover, in addition to liver metastases, other differential diagnoses on US



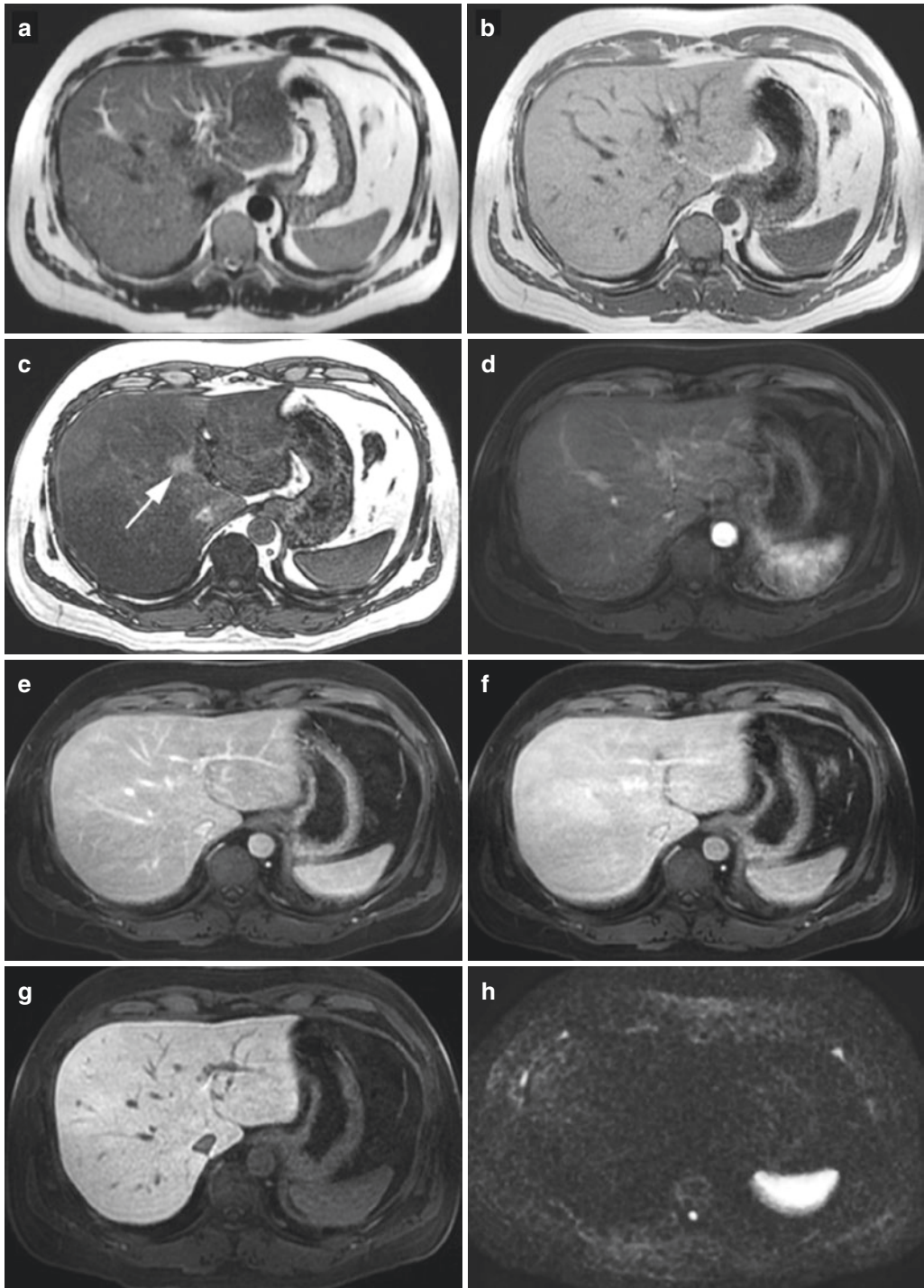


**Fig. 23** Focal fat-sparing area on MRI. T2-weighted (a) and T1-weighted “in phase” (b) images demonstrating no focal lesions. T1-weighted “out-of-phase” (c) image shows a focal hyperintense area at the typical location in segment IV (arrow) on the background of a diffuse liver

dropout of the signal. Dynamic study after contrast administration showing no alteration during the arterial (d), portal (e), delayed (f) and hepatobiliary (g) phases. Diffusion-weighted image (h) revealing no signal restrictions

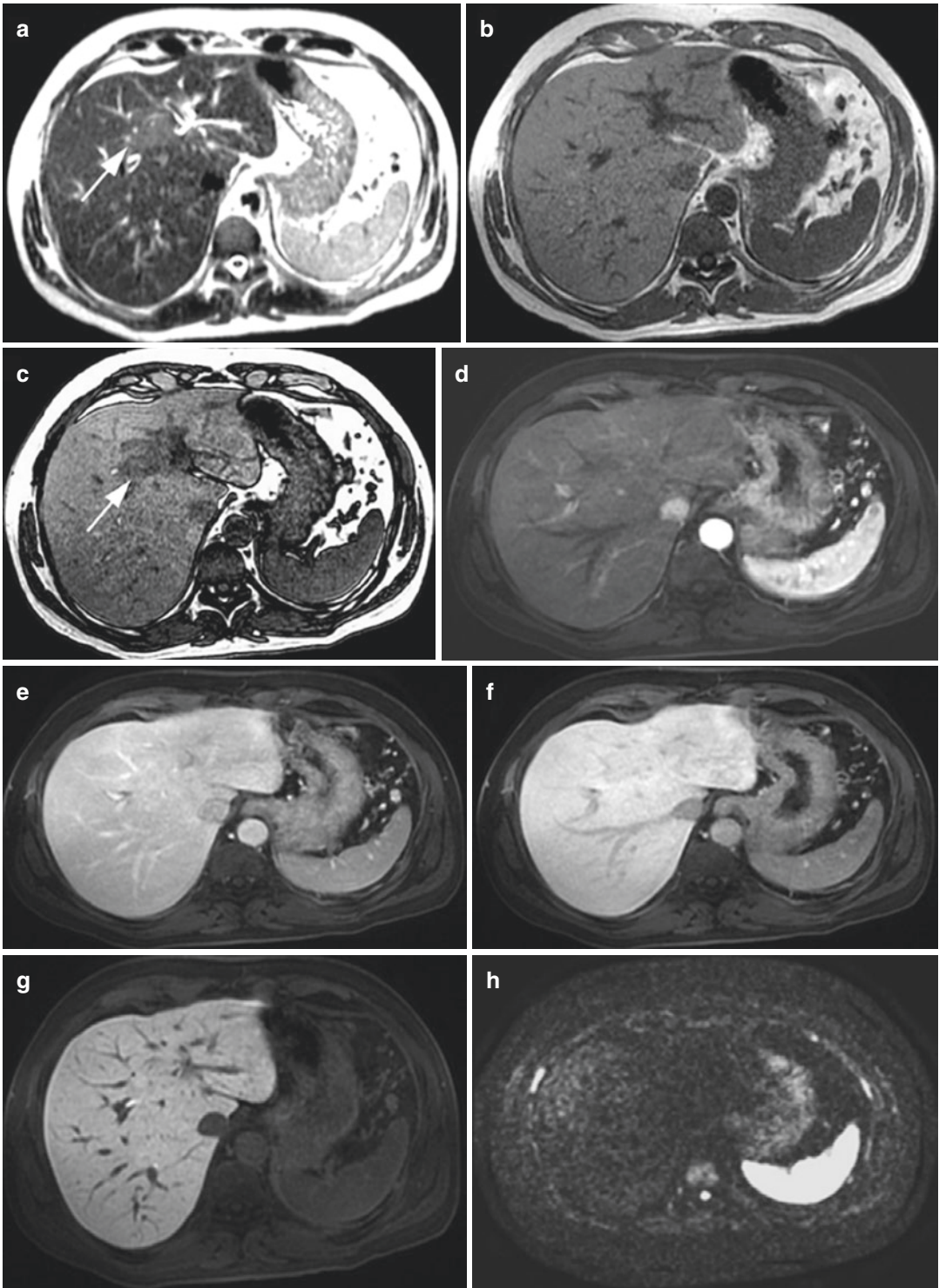


**Fig. 24** Focal steatosis on MRI. T2-weighted image (a) depicts a focal hyperintense area in segment IV (arrow). T1-weighted images showing isointensity to the adjacent parenchyma on the “in-phase” image (b) and hypointensity of the focal area (arrow) on the “out-of-phase” image (c). Dynamic study after contrast administration does not

show signal alteration during the arterial (d), portal (e) and delayed (f) phases, and isointensity to the adjacent parenchyma during the hepatobiliary phase (g). Diffusion-weighted image (h) confirms the absence of diffusion restriction in the area of the focal steatosis

and CT include lymphoma, sarcoidosis, abscesses, candidiasis, hemangiomas and biliary hamartomas. Magnetic resonance imaging is valuable for the correct differential diagnosis of fat deposition in oncological patients, due to the possibility of identifying microscopic fat within the lesions using T1-weighted images exploiting chemical shift artifacts. Moreover, the stability in size of these pseudolesions in the follow-up could indicate the exact diagnosis. In cirrhotic patients, multifocal fat deposition often corresponds to the fat degeneration within multiple RNs.

## References

- Alpern MB, Lawson TL, Foley WD et al (1986) Focal hepatic masses and fatty infiltration detected by enhanced dynamic CT. *Radiology* 158:45–49
- Ames JT, Federle MP, Chopra K (2009) Distinguishing clinical and imaging features of nodular regenerative hyperplasia and large regenerative nodules of the liver. *Clin Radiol* 64:1190–1195
- Angulo P (2002) Nonalcoholic fatty liver disease. *N Engl J Med* 346:1221–1231
- Bhayana D, Kim TK, Jang HJ et al (2010) Hypervascular liver masses on contrast-enhanced ultrasound: the importance of washout. *AJR Am J Roentgenol* 194:977–983
- Bookstein JJ, Cho KJ, Becker GB, Dail D (1982) Arteriportal communications: observations and hypotheses concerning transsinusoidal and transvasal types. *Radiology* 142:581–590
- Boyce CJ, Pickhardt PJ, Kim DH et al (2010) Hepatic steatosis (fatty liver disease) in asymptomatic adults identified by unenhanced low-dose CT. *AJR Am J Roentgenol* 194:623–628
- Brancatelli G, Federle MP, Blachar A, Grazioli L (2001) Hemangioma in the cirrhotic liver: diagnosis and natural history. *Radiology* 219:69–74
- Brancatelli G, Federle MP, Grazioli L et al (2002a) Benign regenerative nodules in Budd Chiari syndrome and other vascular disorders of the liver: radiologic-pathologic and clinical correlations. *Radiographics* 22:847–862
- Brancatelli G, Federle MP, Grazioli L et al (2002b) Large regenerative nodules in Budd-Chiari syndrome and other vascular disorders of the liver: CT and MR findings with clinico-pathologic correlation. *AJR Am J Roentgenol* 178:877–883
- Brancatelli G, Baron RL, Peterson MS, Marsh W (2003) Helical CT screening for hepatocellular carcinoma in patients with cirrhosis: frequency and causes of false-positive interpretation. *Am J Roentgenol* 180:1007–1014
- Brancatelli G, Federle MP, Ambrosini R et al (2007) Cirrhosis: CT and MR imaging evaluation. *Eur J Radiol* 61:57–69
- Brancatelli G, Baron RL, Federle MP et al (2009) Focal confluent fibrosis in cirrhotic liver: natural history studied with serial CT. *AJR Am J Roentgenol* 192:1341–1347
- Brannigan M, Burns PN, Wilson SR (2004) Blood flow patterns in focal liver lesions at microbubble-enhanced US. *Radiographics* 24:921–935
- Breen DJ, Rutherford EE, Stedman B et al (2004) Intrahepatic arteriportal shunting and anomalous venous drainage: understanding the CT features in the liver. *Eur Radiol* 14:2249–2260
- Breitkopf K, Nagy LE, Beier JI et al (2009) Current experimental perspectives on the clinical progression of alcoholic liver disease. *Alcohol Clin Exp Res* 33:1647–1655
- Brunt EM, Tiniakos DG (2002) Pathology of steatohepatitis. *Best Pract Res Clin Gastroenterol* 16:691–707
- Cazals-Hatem D, Vilgrain V, Genin P et al (2003) Arterial and portal circulation and parenchymal changes in Budd-Chiari syndrome: a study in 17 explanted livers. *Hepatology* 37:510–509
- Chen JH, Chai JW, Huang CL et al (1999a) Proximal arteriportal shunting associated with hepatocellular carcinoma: features revealed by dynamic helical CT. *Am J Roentgenol* 172:403–407
- Chen WP, Chen JH, Hwang JI et al (1999b) Spectrum of transient hepatic attenuation differences in biphasic helical CT. *Am J Roentgenol* 172:419–424
- Chen W, DelProposto Z, Wu D et al (2012) Improved Siderotic nodule detection in cirrhosis with susceptibility-weighted magnetic resonance imaging: a prospective study. *PLoS One* 7:e36454
- Chen Y, Pan Y, Shen KR et al (2017) Contrast-enhanced multiple-phase imaging features of intrahepatic mass-forming cholangiocarcinoma and hepatocellular carcinoma with cirrhosis: a comparative study. *Oncol Lett* 14:4213–4219
- Couinaud C (1988) The parabiliary venous system. *Surg Radiol Anat* 10:311–316
- D'Amico G, Garcia-Tsao G, Pagliaro L (2006) Natural history and prognostic indicators of survival in cirrhosis: a systematic review of 118 studies. *J Hepatol* 44:217–231
- De Sousa JM, Portmann B, Williams R (1991) Nodular regenerative hyperplasia of the liver and Budd-Chiari syndrome. Case report, review of the literature and reappraisal of pathogenesis. *J Hepatol* 12:28–35
- Décarie PO, Lepanto L, Billiard JS et al (2011) Fatty liver deposition and sparing: a pictorial review. *Insights Imaging* 2:533–538
- DeLeve LD, Shulman HM, McDonald GB (2002) Toxic injury to hepatic sinusoids: sinusoidal obstruction syndrome (veno-occlusive disease). *Semin Liver Dis* 22:27–42

- Dioguardi Burgio M, Ronot M, Paulatto L et al (2016) Avoiding pitfalls in the interpretation of gadoxetic acid-enhanced magnetic resonance imaging. *Semin Ultrasound CT MR* 37:561–572
- Doo KW, Lee CH, Choi JW et al (2009) “Pseudo washout” sign in high-flow hepatic hemangioma on gadoxetic acid contrast-enhanced MRI mimicking hypervascular tumor. *AJR Am J Roentgenol* 193:W490–W496
- Duran R, Ronot M, Kerbaol A et al (2014) Hepatic hemangiomas: factors associated with T2 shine-through effect on diffusion-weighted MR sequences. *Eur J Radiol* 83:468–478
- Duran R, Ronot M, Di Renzo S et al (2015) Is magnetic resonance imaging of hepatic hemangioma any different in liver fibrosis and cirrhosis compared to normal liver? *Eur J Radiol* 84:816–822
- Elsayes KM, Shaaban AM (2015) Specialty imaging: pitfalls and classic signs of the abdomen and pelvis. Elsevier, Philadelphia, PA
- Francisco FA, de Araújo AL, Oliveira Neto JA, Parente DB (2014) Hepatobiliary contrast agents: differential diagnosis of focal hepatic lesions, pitfalls and other indications. *Radiol Bras* 47:301–309
- Galia M, Taibbi A, Marin D et al (2014) Focal lesions in cirrhotic liver: what else beyond hepatocellular carcinoma? *Diagn Interv Radiol* 20:222–228
- Goodwin MD, Dobson JE, Sirlin CB et al (2011) Diagnostic challenges and pitfalls in MR imaging with hepatocyte-specific contrast agents. *Radiographics* 31:1547–1568
- Gryspeerd S, Van Hoe L, Marchal G, Baert AL (1997) Evaluation of hepatic perfusion disorders with double-phase spiral CT. *Radiographics* 17:337–348
- Hamer OW, Aguirre DA, Casola G et al (2006) Fatty liver: imaging patterns and pitfalls. *Radiographics* 26:1637–1653
- Hanna RF, Aguirre DA, Kased N et al (2008) Cirrhosis-associated hepatocellular nodules: correlation of histopathologic and MR imaging features. *Radiographics* 28:747–769
- Hellekant CH (1976) Vascular complications following needle puncture of the liver. *Acta Radiol* 17:209–222
- Hussain SM, Semelka RC, Mitchell DG (2002) MR imaging of hepatocellular carcinoma. *Magn Reson Imaging Clin N Am* 10:31–52
- International Working Party (1995) Terminology of nodular hepatocellular lesions. *Hepatology* 22:983–993
- Itai Y, Matsui O (1997) Blood flow and liver imaging. *Radiology* 202:306–314
- Itai Y, Matsui O (1999) ‘Nonportal’ splanchnic venous supply to the liver: abnormal findings on CT, US and MRI. *Eur Radiol* 9:237–243
- Itai Y, Saida Y (2002) Pitfalls in liver imaging. *Eur Radiol* 12:1162–1174
- Itai Y, Murata S, Saida Y, Minami M (1994) Central zone and peripheral zone of the liver based on portal and hepatic arterial blood supply; imaging approach to deformity of cirrhotic liver. *Jpn J Clin Radiol* 39:1553–1559
- Itai Y, Murata S, Kurosaki Y (1995) Straight border sign of the liver: spectrum of CT appearances and causes. *Radiographics* 15:1089–1102
- Ito K, Mitchell DG, Gabata T et al (1999) Hepatocellular carcinoma: association with increased iron deposition in the cirrhotic liver at MR imaging. *Radiology* 212:235–224
- Jang HJ, Kim TK, Lim HK et al (2003) Hepatic hemangioma: atypical appearances on CT, MR imaging, and sonography. *AJR Am J Roentgenol* 180:135–141
- Jang HJ, Yu H, Kim TK (2009a) Contrast-enhanced ultrasound in the detection and characterization of liver tumors. *Cancer Imaging* 9:96–103
- Jang HJ, Yu H, Kim TK (2009b) Imaging of focal liver lesions. *Semin Roentgenol* 44:266–282
- Karhunen PJ (1986) Benign hepatic tumours and tumour like conditions in men. *J Clin Pathol* 39:183–188
- Kemper J, Jung G, Poll LW et al (2002) CT and MRI findings of multifocal hepatic steatosis mimicking malignancy. *Abdom Imaging* 27:708–710
- Khalili K, Lan FP, Hanbidge AE et al (2003) Hepatic subcapsular steatosis in response to intraperitoneal insulin delivery: CT findings and prevalence. *AJR Am J Roentgenol* 180:1601–1604
- Kim TK, Jang HJ, Wilson SR (2006) Benign liver masses: imaging with microbubble contrast agents. *Ultrasound Q* 22:31–39
- Kim TK, Lee E, Jang HJ (2015) Imaging findings of mimickers of hepatocellular carcinoma. *Clin Mol Hepatol*:326–343
- Kim B, Byun JH, Kim HJ et al (2016) Enhancement patterns and pseudo-washout of hepatic haemangiomas on gadoxetate disodium-enhanced liver MRI. *Eur Radiol* 26:191–198
- Kobayashi S, Gabata T, Matsui O (2010) Radiologic manifestation of hepatic pseudolesions and pseudotumors in the third inflow area. *Imaging Med* 2:519–528
- Kondo F (2001) Benign nodular hepatocellular lesions caused by abnormal hepatic circulation: etiological analysis and introduction of a new concept. *J Gastroenterol Hepatol* 16:1319–1328
- Krinsky GA, Lee VS, Nguyen MT et al (2000) Siderotic nodules at MR imaging: regenerative or dysplastic? *J Comput Assist Tomogr* 24:773–776
- Krinsky GA, Lee VS, Nguyen MT et al (2001) Siderotic nodules in the cirrhotic liver at MR imaging with explant correlation: no increased frequency of dysplastic nodules and hepatocellular carcinoma. *Radiology* 218:47–53
- Krinsky GA, Zivin SB, Thorner KM et al (2002) Low grade siderotic dysplastic nodules: determination of premalignant lesions on the basis of vasculature phenotype. *Acad Radiol* 9:336–341
- Kroncke TJ, Taupitz M, Kivelitz D et al (2000) Multifocal nodular fatty infiltration of the liver mimicking metastatic disease on CT: imaging findings and diagnosis using MR imaging. *Eur Radiol* 10:1095–1100
- Kudo M (2009) Multistep human hepatocarcinogenesis: correlation of imaging with pathology. *J Gastroenterol* 19:112–118

- Lee SJ, Lim JH, Lee WJ et al (1997) Transient subsegmental hepatic parenchymal enhancement on dynamic CT: a sign of postbiopsy arterioportal shunt. *J Comput Assist Tomogr* 21:355–360
- Makhlouf HR, Ishak KG (2002) Sclerosed hemangiomas and sclerosing cavernous hemangioma of the liver: a comparative clinicopathologic and immunohistochemical study with emphasis on the role of mast cells in their histogenesis. *Liver* 22:70–78
- Marrero JA, Ahn J, Rajender Reddy K (2014) American College of Gastroenterology. ACG clinical guideline: the diagnosis and management of focal liver lesions. *Am J Gastroenterol* 109:1328–1347
- Martin J, Puig J, Darnell A, Donoso L (2002) Magnetic resonance of focal liver lesions in hepatic cirrhosis and chronic hepatitis. *Semin Ultrasound CT MR* 23:62–78
- Mastropasqua M, Kanematsu M, Leonardou P et al (2004) Cavernous hemangiomas in patients with chronic liver disease: MR imaging findings. *Magn Reson Imaging* 22:15–18
- Mathiesen UL, Franzen LE, Aselius H et al (2002) Increased liver echogenicity at ultrasound examination reflects degree of steatosis but not of fibrosis in asymptomatic patients with mild/moderate abnormalities of liver transaminases. *Dig Liver Dis* 34:516–522
- Mathieu D, Paret M, Mahfouz AE et al (1997) Hyperintense benign liver lesions on spin-echo T1-weighted MR images: pathologic correlations. *Abdom Imaging* 22:410–417
- Mathieu D, Luciani A, Achab A et al (2001) Hepatic Pseudolesions. *Gastroenterol Clin Biol* 25:B158–B166
- Matsui O, Kadoya M, Takahashi S et al (1995) Focal sparing of segment IV in fatty livers shown by sonography and CT: correlation with aberrant gastric venous drainage. *AJR Am J Roentgenol* 164:1137–1140
- Mitchell DG, Rubin R, Siegelman ES et al (1991) Hepatocellular carcinoma within siderotic regenerative nodules: appearance as a nodule within a nodule on MR images. *Radiology* 178:101–103
- Mittal S, El-Serag HB (2013) Epidemiology of hepatocellular carcinoma: consider the population. *J Clin Gastroenterol* 47.(suppl):S2–S6
- Motosugi U, Ichikawa T, Sou H et al (2010) Distinguishing hypervascular pseudolesions of the liver from hypervascular hepatocellular carcinomas with gadoteric acid-enhanced MR imaging. *Radiology* 256(1):151–158
- Murata S, Itai Y, Asato M et al (1995) Effect of temporary occlusion of the hepatic vein on dual blood in the liver: evaluation with spiral CT. *Radiology* 197:351–356
- Nicolau C, Brú C (2004) Focal liver lesions: evaluation with contrast-enhanced ultrasonography. *Abdom Imaging* 29:348–359
- O'Malley ME, Takayama Y, Sherman M (2005) Outcome of small (10–20 mm) arterial phase-enhancing nodules seen on triphasic liver CT in patients with cirrhosis or chronic liver disease. *Am J Gastroenterol* 100:1523–1528
- Ohtomo K, Baron RL, Dodd GD 3rd et al (1993a) Confluent hepatic fibrosis in advanced cirrhosis: appearance at CT. *Radiology* 188:31–35
- Ohtomo K, Baron RL, Dodd GD 3rd et al (1993b) Confluent hepatic fibrosis in advanced cirrhosis: evaluation with MR imaging. *Radiology* 189:871–874
- Okuda K, Musha H, Nakajima Y et al (1978) Frequency of intrahepatic arteriovenous fistula as a sequela to percutaneous needle puncture of the liver. *Gastroenterology* 74:1204–1207
- Park YN, Kim M-J (2011) Hepatocarcinogenesis: imaging-pathologic correlation. *Abdom Imaging* 36:232–243
- Park YS, Lee CH, Kim BH et al (2013) Using Gd-EOB-DTPA-enhanced 3-T MRI for the differentiation of infiltrative hepatocellular carcinoma and focal confluent fibrosis in liver cirrhosis. *Magn Reson Imaging* 31:1137–1142
- Prasad SR, Wang H, Rosas H et al (2005) Fat-containing lesions of the liver: radiologic-pathologic correlation. *Radiographics* 25:321–333
- Renzulli M, Lucidi V, Mosconi C et al (2011) Large regenerative nodules in a patient with Budd-Chiari syndrome after TIPS positioning while on the liver transplantation list diagnosed by Gd-EOB-DTPA MRI. *Hepatobiliary Pancreat Dis Int* 10:439–442
- Ronot M, Dioguardi Burgio M, Purcell Y et al (2017) Focal lesions in cirrhosis: not always HCC. *Eur J Radiol* 93:157–168
- Sadek AG, Mitchell DG, Siegelman ES et al (1995) Early hepatocellular carcinoma that develops within macrorregenerative nodules: growth rate depicted at serial MR imaging. *Radiology* 195:753–756
- Scheuer PJ, Lefkowitz JH (2000) Fatty liver and lesions in the alcoholic. In: *Liver biopsy interpretation*, 6th edn. Saunders, Philadelphia, PA, pp 111–129
- Shimizu A, Ito K, Koike S et al (2003) Cirrhosis or chronic hepatitis: evaluation of small (<or=2-cm) early-enhancing hepatic lesions with serial contrast-enhanced dynamic MR imaging. *Radiology* 226:550–555
- Siegelman ES, Chauhan A (2014) MR characterization of focal liver lesions. *Magn Reson Imaging Clin N Am* 22:295–313
- Siegelman ES, Mitchell DG, Semelka RC (1996) Abdominal iron deposition: metabolism, MR findings, and clinical importance. *Radiology* 199:13–22
- Sohn J, Siegelman E, Osiason A (2001) Unusual patterns of hepatic steatosis caused by the local effect of insulin revealed on chemical shift MR imaging. *AJR Am J Roentgenol* 176:471–474
- Steiner PE (1959) Nodular regenerative hyperplasia of the liver. *Am J Pathol* 35:943–953
- Stromeyer FW, Ishak KG (1981) Nodular transformation (nodular "regenerative" hyperplasia) of the liver. A clinicopathologic study of 30 cases. *Hum Pathol* 12:60–71
- Sun HY, Lee JM, Shin CI et al (2010) Gadoteric acid-enhanced magnetic resonance imaging for differentiating small hepatocellular carcinomas (< or =2 cm

- in diameter) from arterial enhancing pseudolesions: special emphasis on hepatobiliary phase imaging. *Investig Radiol* 45(2):96–103
- Takayasu K, Muramatsu Y, Moriyama N et al (1994) Radiological study of idiopathic Budd-Chiari syndrome complicated by hepatocellular carcinoma. A report of four cases. *Am J Gastroenterol* 89:249–253
- Tamada T, Ito K, Yamamoto A et al (2011) Hepatic hemangiomas: evaluation of enhancement patterns at dynamic MRI with gadoxetate disodium. *AJR Am J Roentgenol* 196:824–830
- Tanaka M, Wanless IR (1998) Pathology of the liver in Budd-Chiari syndrome: portal vein thrombosis and the histogenesis of veno-centric cirrhosis, veno-portal cirrhosis, and large regenerative nodules. *Hepatology* 27:488–496
- Terada T, Nakanuma Y (1989) Survey of iron-accumulative macroregenerative nodules in cirrhotic livers. *Hepatology* 10:851–854
- Terada T, Kadoya M, Nakanuma Y, Matsui O (1990) Iron-accumulating adenomatous hyperplastic nodule with malignant foci in the cirrhotic liver histopathologic, quantitative iron, and magnetic resonance imaging in vitro studies. *Cancer* 65:1994–2000
- Vilgrain V, Lewin M, Vons C et al (1999) Hepatic nodules in Budd-Chiari syndrome: imaging features. *Radiology* 210:443–450
- Vilgrain V, Lagadec M, Ronot M (2016) Pitfalls in liver imaging. *Radiology* 278:34–51
- Wachsberg RH, Bahramipour P, Sofocleous CT, Barone A (2002) Hepatofugal flow in the portal venous system: pathophysiology, imaging findings, and diagnostic pitfalls. *Radiographics* 22:123–140
- Wanless IR (1990) Micronodular transformation (nodular regenerative hyperplasia) of the liver: a report of 64 cases among 2,500 autopsies and a new classification of benign hepatocellular nodules. *Hepatology* 11:787–797
- Wanless IR, Mawdsley C, Adams R (1985) On the pathogenesis of focal nodular hyperplasia of the liver. *Hepatology* 5:1194–1200
- Wilson SR, Jang HJ, Kim TK et al (2008) Real-time temporal maximum-intensity-projection imaging of hepatic lesions with contrast-enhanced sonography. *AJR Am J Roentgenol* 190:691–695
- Yoshimitsu K, Honda H, Kuroiwa T et al (1999) Pseudolesions of the liver possibly caused by focal rib compression: analysis based on hemodynamic change. *AJR Am J Roentgenol* 172:645–649
- Yoshimitsu K, Honda H, Kuroiwa T et al (2001) Unusual hemodynamics and pseudolesions of the noncirrhotic liver at CT. *Radiographics* 21:S81–S96
- Yu JS, Kim KW, Sung KB et al (1997) Small arterial-portal venous shunts: a cause of pseudolesions at hepatic imaging. *Radiology* 203:737–742
- Yu JS, Kim KW, Yeong MG et al (2000) Non tumorous hepatic arterial-portal venous shunts: MR imaging findings. *Radiology* 217:750–756
- Zhang J, Krinsky GA (2004) Iron-containing nodules of cirrhosis. *NMR Biomed* 17:459–464